Politecnico di Torino

Politecnico di Torino

Master Degree Course Electronics Engineering

AcademicYear 2025-2026
Graduation Session July 2026

Thesis Title

"Automated Detection of Brugada Syndrome Type 1 Using Digitized ECG Signal Analysis and Neural Networks"

Supervisor:
Prof. PASERO EROS GIAN ALESSANDRO

Co-Supervisor:
Prof. RANDAZZO VINCENZO

Candidate:
MUNEEB AHMED

Acknowledgements

I would like to begin by sincerely thanking my professor and supervisor, Prof. Pasero Gian Alessandro, along with my co-supervisor, Randazzo Vincenzo, for their constant support, valuable guidance, and availability throughout the preparation of my thesis. Their encouragement and expertise played a crucial role in the successful completion of this work.

I am also very grateful to Mr.Alessandro Casella for his generous assistance during my thesis journey. His willingness to help whenever I needed support and his willingness to go beyond expectations made a significant difference in this process.

I would also like to thank my colleagues Muhammad Hammad Rauf and Waqas Khan who contributed additional digitized ECG datasets, which helped expand the data available for neural network training. Their support improved the diversity and size of the dataset used in this work.

Lastly, I would like to express my heartfelt appreciation to my family for their unconditional support throughout my life. I am especially grateful to my parents for their continuous encouragement during my academic years and while conducting research and writing this thesis. I am truly grateful to my father, Shafiq Ahmed, who has always been a strong pillar of support in my life. I also would like to thank my mother, Shabana, whose constant encouragement and comforting words during challenging times mean so much to me.

I express my deepest gratitude to all of them from the bottom of my heart.

Abstract

Brugada syndrome is a hereditary disease characterized by abnormal heart rhythm that is at high risk of ventricular arrhythmia and sudden cardiac death. In terms of ECG changes, Type 1 Brugada pattern is considered to be the most clinically relevant among all other types because it reflects the typical ECG pattern. It is important to accurately distinguish between this type of pattern, but it is not always easy since there are some minor waveform differences, sporadic nature, and similarity with other ECG changes.

This thesis presents the design of an end-to-end pipeline that is intended for the automatic detection of Brugada Syndrome Type 1 based on digitalization of electrocardiogram (ECG) signals via deep learning. It should be noted that original ECG data were obtained from sources where these signals had a form of a PDF document that could not be used directly for machine learning models. As a result, in order to process such a dataset, the first step involved the digitization of PDF ECG data via ECGD program with the creation of XLSX files with numerical series. A dataset with 1,041 XLSX files has been created.

Afterward, the ECG datasets underwent preprocessing in order to extract leads V1, V2, and V3 that have clinical importance in the diagnosis of Brugada Type 1 syndrome. Signal interpolation was performed in a sampling frequency of 500 Hz and S-peak-based windowing was done to retain the QRS-ST-T portion. The preprocessed dataset included 2377 ECG windows, distributed in to the training, validation and testing set.

A CNN-BiLSTM-Attention architecture was designed for the purpose of discriminating between non-Brugada Syndrome (BrS) and Definite/Type 1 BrS ECG segments using binary classification. The use of convolutions helped extract the local features of the waveform; bidirectional LSTMs facilitated the capturing of temporal dynamics; and attention improved explainability. Class imbalances were managed by sampling weights while the optimal decision threshold was identified based on the ROC curve using Youden's j index.

The developed framework achieved an average accuracy of 82% on the test dataset. In the case of Definitive / Brugada Type 1 class, the precision, recall, and F1 scores were 0.89, 0.85, and 0.87 respectively. The AUC of the ROC was 0.849, while the optimal cutoff point was around 0.39. The above results demonstrate that it is possible to use digitalized ECG data in combination with machine learning techniques for automatic classification of patients with Brugada Syndrome Type 1. However, more research is needed, including the creation of bigger datasets, balancing classes, external validation, and expert review.

The method proposed here could form a reasonable starting point for future study relating to the diagnosis of electrocardiogram based (ECG) conditions.

List of Abbreviations

Abbreviation	Full Form
ECG	Electrocardiogram
BrS	Brugada Syndrome
BrS Type 1	Brugada Syndrome Type 1
Non-BrS	Non-Brugada Syndrome
CNN	Convolutional Neural Network
BiLSTM	Bidirectional Long Short-Term Memory
LSTM	Long Short-Term Memory
AI	Artificial Intelligence
ML	Machine Learning
DL	Deep Learning
XLSX	Microsoft Excel Spreadsheet Format
PDF	Portable Document Format
ECGD	ECG Digitization Software
ADC	Analog-to-Digital Conversion
ROC	Receiver Operating Characteristic
AUC	Area Under the Curve
ROC-AUC	Receiver Operating Characteristic Area Under Curve
F1-score	Harmonic Mean of Precision and Recall
TP	True Positive
TN	True Negative
FP	False Positive
FN	False Negative
TPR	True Positive Rate
FPR	False Positive Rate
AUPRC	Area Under the Precision-Recall Curve
Hz	Hertz
ms	Millisecond
mV	Millivolt
ST Segment	Segment between QRS complex and T wave
QRS	Ventricular Depolarization Complex

Table of Contents

List of Tables

List of Figures

Chapter 1

Introduction

1.1 Background of Cardiovascular Diseases

Cardiovascular diseases remain one of the leading causes of mortality worldwide and represent a major global public health challenge [1]. These diseases include a wide range of conditions affecting the heart and blood vessels, such as coronary artery disease, heart failure, arrhythmias, inherited cardiac disorders, and sudden cardiac death. Among these conditions, rhythm-related disorders are particularly dangerous because they may occur suddenly and without obvious warning signs. In some patients, the first clinical manifestation of an underlying electrical heart disorder may be syncope, ventricular fibrillation, or sudden cardiac death [2].

The heart functions through a highly coordinated electrical conduction system. Electrical impulses originate in the sinoatrial node and propagate through the atria, atrioventricular node, His-Purkinje system, and ventricles. Any disturbance in this electrical activity may produce abnormal rhythms known as arrhythmias. Some arrhythmias are benign, while others can be life-threatening [3, 4]. The early identification of dangerous arrhythmogenic conditions is therefore essential for prevention, treatment, and risk management.

The electrocardiogram, commonly known as the ECG, is one of the most widely used tools for assessing cardiac electrical activity. It is non-invasive, inexpensive, fast, and clinically informative [5]. ECG recordings allow clinicians to evaluate heart rhythm, conduction intervals, waveform morphology, and repolarization abnormalities. Because of these advantages, ECG analysis remains central to the diagnosis of many cardiac diseases, including inherited arrhythmia syndromes [6].

However, ECG interpretation can be challenging. Some pathological patterns are subtle, intermittent, or hidden under normal baseline conditions. This is particularly true for inherited electrical diseases such as Brugada Syndrome, where

the diagnostic ECG pattern may not always be visible [7]. These challenges motivate the development of automated and intelligent systems capable of supporting clinicians in ECG interpretation [8].

1.2 Sudden Cardiac Death and Inherited Arrhythmias

Sudden cardiac death is one of the most serious outcomes of cardiac electrical instability [9]. It usually occurs due to malignant ventricular arrhythmias such as ventricular tachycardia or ventricular fibrillation. In many cases, sudden cardiac death occurs in individuals with known structural heart disease; however, it may also occur in patients with apparently normal cardiac structure [10]. In such cases, inherited arrhythmogenic disorders are often suspected.

Inherited arrhythmia syndromes are caused by abnormalities in ion channels or proteins involved in cardiac electrical conduction [11]. These disorders may not produce structural changes visible on imaging studies, making them difficult to identify through conventional diagnostic approaches. Instead, their diagnosis often depends on ECG abnormalities, clinical history, family history, genetic testing, and provocation testing.

Brugada Syndrome belongs to this group of inherited arrhythmogenic disorders [12]. It is clinically important because it is associated with an increased risk of ventricular fibrillation and sudden cardiac death, particularly in younger individuals and in patients without structural heart disease. The disease is therefore not only a cardiological problem but also a diagnostic and preventive challenge.

In the context of this thesis, the focus is not on all inherited arrhythmia disorders, nor even on all ECG patterns associated with Brugada Syndrome. The specific focus is on the automated detection of Brugada Syndrome Type 1, also referred to in this project as the Definitive class. This distinction is essential because Type 1 is the diagnostically significant ECG pattern and represents the main clinical target of the proposed machine learning model [13].

1.3 Overview of Brugada Syndrome

Brugada Syndrome is an inherited cardiac electrical disorder associated with abnormal ventricular depolarization and repolarization[4]. It is commonly described as a channelopathy because it is often related to dysfunction of cardiac ion channels, especially sodium channels. The disorder may be associated with genetic variants, including mutations affecting the cardiac sodium channel gene, although not all patients have identifiable genetic mutations.

The syndrome is characterized by specific ECG patterns, especially in the right precordial leads. These leads, V1, V2, and V3, are positioned over the right anterior chest and are particularly important for identifying abnormalities related to the right ventricular outflow tract [14]. The ECG manifestations of Brugada Syndrome may vary over time and can be influenced by fever, autonomic tone, medications, electrolyte disturbances, and pharmacological provocation.

Brugada ECG patterns are commonly classified into different types. Type 1 is the coved-type pattern and is considered diagnostic when present under appropriate clinical conditions. Type 2 and Type 3 patterns may raise suspicion but are not considered definitively diagnostic on their own. This distinction is very important for this thesis. The proposed work does not aim to detect every possible Brugada-like ECG abnormality. Instead, it focuses on the detection of Type 1 Brugada pattern, which corresponds to the Definitive class in the dataset [15].

Because Type 1 Brugada pattern is associated with potentially life-threatening arrhythmias, its accurate detection is clinically significant. Missing a Type 1 case may delay diagnosis and risk stratification. On the other hand, false classification of non-Brugada ECGs as Type 1 may lead to unnecessary concern or further testing. Therefore, an automated system must be evaluated carefully using suitable performance metrics such as precision, recall, F1-score, confusion matrix analysis, and ROC-based threshold optimization [16].

1.4 Importance of Brugada Syndrome Type 1

Brugada Syndrome Type 1 is the most clinically important ECG pattern associated with Brugada Syndrome because it is the definitive diagnostic pattern. It is typically characterized by coved ST-segment elevation in the right precordial leads, followed by a negative T wave. These morphological features are usually evaluated in leads V1, V2, and V3. The presence of this pattern may indicate an increased risk of malignant ventricular arrhythmias [17].

The importance of Type 1 Brugada pattern arises from its diagnostic and prognostic relevance. Unlike suspicious or borderline patterns, the Type 1 pattern is directly linked with clinical diagnosis. Therefore, automated recognition of Type 1 morphology has practical value in clinical screening and decision support [18]. In this thesis, the term Definitive is used to represent ECG files labeled as Brugada Type 1, while Non-BrS represents ECG files without the definitive Type 1 Brugada pattern.

A major difficulty is that Type 1 Brugada pattern can be intermittent. Some patients may not show the diagnostic pattern during a routine baseline ECG. [7] In such cases, clinicians may use pharmacological provocation tests, such as sodium channel blocker challenge, to reveal concealed Brugada patterns. However, these

procedures require clinical supervision and may carry risks. This creates a strong motivation for non-invasive computational tools that can help identify subtle or hidden ECG features from baseline recordings.

The use of artificial intelligence in this context is promising because neural networks can learn complex morphological patterns that may not be easily captured by manual measurements alone. However, the success of such models depends strongly on the quality of the ECG data, preprocessing strategy, model architecture, and evaluation method. This thesis therefore develops a complete pipeline starting from ECG digitization and ending with neural network-based classification. [19]

1.5 Role of ECG in Brugada Syndrome Diagnosis

The ECG is central to Brugada Syndrome diagnosis because the disorder primarily manifests as an electrical abnormality rather than a structural cardiac defect. A standard ECG records the heart's electrical activity from multiple leads, allowing the analysis of waveform morphology across different anatomical perspectives. In Brugada Syndrome, the right precordial leads are particularly relevant because they reflect electrical activity near the right ventricular outflow tract [7].

A typical ECG waveform consists of the P wave, PR interval, QRS complex, ST segment, and T wave. In Brugada Syndrome Type 1, the most relevant region is the QRS-ST-T complex. The diagnostic morphology appears around the end of the QRS complex and the beginning of the ST segment, where coved ST elevation and subsequent T-wave inversion may be observed [14]. This means that accurate detection requires preserving the morphology of the signal around the QRS complex, J-point, ST segment, and T wave.

In this thesis, special attention is given to leads V1, V2, and V3 because these leads are clinically most relevant for Type 1 Brugada detection. The implemented preprocessing pipeline extracts these leads from digitized XLSX files and processes them as multi-lead ECG windows. This approach allows the model to learn not only individual waveform morphology but also relationships among the right precordial leads [20].

The ECG data used in this work was originally provided in PDF format, which means the ECG waveforms were available as visual traces rather than numerical time-series signals. This created an additional engineering challenge. Before applying signal processing and machine learning, the ECG traces had to be digitized and converted into structured numerical form. This digitization stage is one of the major contributions of the thesis.

1.6 Challenges in Manual ECG Interpretation

Manual ECG interpretation requires clinical expertise and careful analysis of waveform morphology. Although experienced cardiologists can identify characteristic Brugada patterns, several factors make the diagnosis challenging. The Type 1 pattern may be subtle, intermittent, or influenced by external conditions. Moreover, other ECG abnormalities, such as right bundle branch block or early repolarization patterns, may resemble Brugada-like morphology and create diagnostic ambiguity.

Inter-observer variability is another important challenge. Different clinicians may interpret borderline ECG patterns differently, especially when the ST-segment shape is not clearly diagnostic. Small differences in electrode placement can also influence the visibility of Brugada patterns. Since the right precordial leads are particularly sensitive to lead position, slight variations may affect the appearance of ST elevation.

In addition, ECGs stored in PDF or scanned format introduce technical limitations. Such ECGs are useful for visual inspection but not directly suitable for computational analysis. Important numerical properties, such as amplitude values and timing intervals, are not directly available. Therefore, the use of machine learning requires an additional step of converting analog ECG traces into digital signals.

These challenges highlight the need for automated ECG analysis systems. A well-designed machine learning model can assist clinicians by providing objective classification support. However, such systems should not be viewed as replacements for clinical judgment. Instead, they can serve as decision-support tools that highlight possible Type 1 Brugada patterns and support further clinical evaluation.

1.7 Motivation for AI-Based Brugada Type 1 Detection

Artificial intelligence has become increasingly important in biomedical signal analysis. Deep learning models are especially useful for ECG classification because they can automatically learn features from raw or minimally processed signals [21]. Unlike traditional methods, which often rely on manually engineered features, neural networks can learn complex waveform patterns directly from data.

The motivation for using AI in this thesis is based on three main factors. First, Brugada Syndrome Type 1 has important clinical consequences, and early detection may support timely diagnosis and risk assessment [22]. Second, the ECG features associated with Type 1 Brugada pattern may be subtle and difficult to identify manually, especially in noisy or digitized recordings. Third, the availability of digitized ECG signals enables the use of modern machine learning techniques for

automated classification.

The model implemented in this thesis follows the concept of a CNN-BiLSTM-Attention architecture inspired by the MeMeA 2025 Brugada classification approach. The convolutional layers are used to extract local waveform features, the bidirectional LSTM layers are used to learn temporal dependencies, and the attention mechanism is used to highlight relevant time regions of the ECG signal. The model is adapted for binary classification between Non-BrS and Definitive / Brugada Type 1. [23]

The motivation is therefore not only to build a classifier but to construct a complete pipeline. This pipeline includes ECG digitization, dataset cleaning, signal preprocessing, S-peak-based window extraction, neural network training, threshold optimization, and interpretability through attention maps. This end-to-end structure makes the thesis both clinically relevant and technically meaningful.

1.8 Problem Statement

The central problem addressed in this thesis is the automated detection of Brugada Syndrome Type 1 / Definitive ECG pattern from digitized ECG signals [4]. The original ECG recordings were provided in PDF format and were therefore not directly usable for signal processing or machine learning. A complete workflow was required to convert these ECG traces into digital numerical signals, organize them into labeled classes, preprocess the signals, and train a neural network model.

The problem can be divided into two major components. The first component is data preparation. ECGs available as PDF reports must be digitized into numerical form. The resulting files must then be cleaned, labeled, and validated. In this work, the raw combined digitized dataset contained 1041 XLSX ECG files, from which 784 labeled files were successfully mapped into the final cleaned dataset, while unlabeled files were discarded. The cleaned dataset was organized into two classes: Definitive and Non-BrS.

The second component is classification. The neural network must learn to distinguish ECG windows belonging to the Definitive Type 1 Brugada class from Non-BrS windows. This is challenging because the dataset is imbalanced, ECG morphology varies across patients, and digitization may introduce noise or signal irregularities. Furthermore, the clinically relevant features are localized around the QRS-ST-T region, making correct window extraction and lead selection essential.

Therefore, this thesis addresses the following research question:

> How can ECG records originally available in PDF format be digitized, processed, and used to train a neural network capable of detecting Brugada Syndrome Type 1 / Definitive ECG patterns from right precordial ECG leads?

1.9 Research Objectives

The main objective of this thesis is to develop an end-to-end artificial intelligence pipeline for the detection of Brugada Syndrome Type 1 / Definitive ECG pattern using digitized ECG signals.

The specific objectives are as follows:

1. To convert ECG records originally available in PDF format into structured digital ECG signals using ECG digitization methods.
2. To construct and clean a labeled ECG dataset suitable for machine learning, separating Definitive / Brugada Type 1 cases from Non-BrS cases.
3. To extract clinically relevant ECG leads, especially V1, V2, and V3, from the digitized XLSX files.
4. To preprocess ECG signals through interpolation, cleaning, baseline correction, and S-peak-based segmentation.
5. To extract fixed-length ECG windows around the S-peak, preserving the QRS-ST-T region relevant to Brugada Type 1 morphology [7, 24].
6. To implement a CNN-BiLSTM-Attention neural network architecture inspired by the MeMeA 2025 Brugada classification model [23].
7. To address class imbalance using suitable training strategies such as weighted sampling.
8. To optimize the decision threshold using validation-based ROC analysis and Youden's J statistic [25].
9. To evaluate the trained model using accuracy, precision, recall, F1-score, ROC curve, confusion matrix, and attention visualization.
10. To interpret the results in relation to clinical relevance, dataset limitations, and future improvements.

1.10 Scope of the Thesis

The scope of this thesis is limited to the detection of Brugada Syndrome Type 1, also referred to as the Definitive class [4, 26, 19]. The thesis does not aim to perform complete clinical diagnosis of all Brugada Syndrome variants. It does not focus on Type 2, Type 3, genetic analysis, risk stratification, or treatment

decision-making. Instead, the work is focused on binary ECG classification between Definitive Brugada Type 1 and Non-BrS.

The ECG signals used in this thesis are derived from digitized clinical ECG records. The main leads used for model development are V1, V2, and V3 because of their clinical relevance to Brugada Type 1 detection [7, 24]. Although other leads may contain additional information, the present work focuses on the right precordial leads in line with the diagnostic importance of these leads.

The thesis includes both data engineering and machine learning components. The data engineering component involves ECG digitization, XLSX dataset construction, label mapping, dataset cleaning, and quality control. The machine learning component involves signal preprocessing, S-peak detection, ECG window extraction, neural network implementation, model training, threshold optimization, and evaluation.

The proposed system should be understood as a research prototype and not as a final clinical diagnostic tool. Clinical use would require larger datasets, external validation, prospective testing, and expert cardiologist review.

1.11 Significance of the Study

The significance of this study can be summarized through the following key points:

- This thesis focuses specifically on Brugada Syndrome Type 1 / Definitive pattern, which is the clinically diagnostic ECG pattern and the most important target for automated detection [4, 26, 19].
- The work develops an end-to-end pipeline beginning from PDF ECG records, which are converted into digital XLSX time-series signals before machine learning is applied.
- The study demonstrates how real-world ECG data, originally stored in a non-computational format, can be transformed into a structured dataset suitable for artificial intelligence.
- The dataset cleaning process improves reliability by removing unlabeled or inconsistent files and organizing labeled ECGs into Definitive and Non-BrS classes.
- The preprocessing pipeline extracts V1, V2, and V3 leads and generates S-peak-centered ECG windows that preserve the clinically relevant QRS-ST-T region [7, 24].

- The neural network model combines convolutional, recurrent, and attention-based components to learn both local waveform morphology and temporal dependencies [27, 28, 29].
- The use of attention maps provides a degree of interpretability by showing which ECG regions contribute to the model's classification decision.
- The final model evaluation demonstrates the feasibility of automated Brugada Type 1 detection using digitized ECG signals [23, 30, 31].
- The study contributes to AI-assisted cardiology by addressing not only classification but also the practical problem of converting PDF ECG records into machine-learning-ready data.

1.12 Main Contributions

This thesis provides several technical and clinical contributions.

First, it presents a digitization workflow for converting ECG records from PDF format into numerical XLSX files. This is an important contribution because many clinical ECG archives store records as PDF reports rather than raw digital signals. By digitizing these ECGs, the thesis creates a bridge between clinical documentation and machine learning analysis.

Second, it constructs a cleaned and labeled ECG dataset. The raw combined dataset contained ECG files from multiple sources. These files were cleaned, mapped to clinical labels, and organized into Definitive and Non-BrS folders. This step was essential for supervised learning.

Third, it develops a preprocessing pipeline for ECG signal preparation. This includes extraction of V1, V2, and V3 leads, interpolation to a standard sampling rate, ECG cleaning, R-peak and S-peak detection, and extraction of 850 ms windows around the S-peak. These windows preserve the region where Brugada Type 1 morphology is most relevant [7, 24].

Fourth, it implements a CNN-BiLSTM-Attention neural network for binary classification. The architecture is inspired by the MeMeA 2025 Brugada classification model [23] but adapted to the available dataset and binary detection objective. The final model outputs predictions for Non-BrS and Definitive / Brugada Type 1 classes.

Fifth, it evaluates the model using multiple metrics and visual outputs. The evaluation includes classification report, confusion matrix, ROC curve, threshold optimization, sampling ECDF, and attention map visualization [25, 32]. These outputs provide both quantitative and interpretability-based analysis.

1.13 Thesis Organization

The remainder of this thesis is organized as follows.

Chapter 2 – Literature Review presents the clinical background of Brugada Syndrome, ECG fundamentals, Type 1 Brugada morphology, advanced ECG features, and artificial intelligence approaches for ECG classification. It also reviews relevant research papers and identifies the research gap addressed by this thesis.

Chapter 3 – ECG Digitization and Dataset Construction describes the conversion of PDF ECG records into digital XLSX signals. It explains the ECGD-based digitization workflow, analog-to-digital signal reconstruction concept, dataset construction, label mapping, dataset cleaning, and quality control.

Chapter 4 – Preprocessing and Neural Network Methodology explains the computational pipeline used after dataset construction. It covers XLSX signal loading, V1–V3 lead extraction, interpolation to 500 Hz, ECG cleaning, R/S-peak detection, 850 ms window extraction, dataset splitting, class imbalance handling, model architecture, training strategy, and threshold optimization.

Chapter 5 – Results and Evaluation presents the experimental results of the neural network model. It includes the classification report, confusion matrix, ROC curve, threshold analysis, attention maps, sampling distribution analysis, and interpretation of model performance.

Chapter 6 – Discussion interprets the results in clinical and technical contexts. It discusses the strengths and limitations of the proposed pipeline, the impact of class imbalance, the role of attention mechanisms, comparison with related work, and practical considerations for future clinical application.

Chapter 7 – Conclusion and Future Work summarizes the thesis contributions and outlines future directions, including larger datasets, multi-class classification, additional ECG leads, external validation, and real-time ECG monitoring.

1.14 Chapter Summary

This chapter introduced the motivation, background, and objectives of the thesis. The central focus of the work is the automated detection of Brugada Syndrome Type 1 / Definitive ECG pattern, not general Brugada Syndrome classification. The chapter explained the clinical importance of Type 1 Brugada pattern, the role of ECG in diagnosis, the challenges of manual interpretation, and the need for AI-based decision support.

The chapter also introduced the main technical problem: ECG records were originally available in PDF format and had to be digitized into numerical signals

before machine learning could be applied. The proposed thesis therefore follows an end-to-end approach that includes ECG digitization, dataset cleaning, signal preprocessing, neural network implementation, and model evaluation.

The next chapter reviews the clinical and technical literature related to Brugada Syndrome Type 1, ECG analysis, and artificial intelligence-based ECG classification.

Chapter 2

Literature Review

2.1 Introduction

This chapter presents a comprehensive review of the clinical, electrocardiographic, signal processing, and artificial intelligence literature related to the automated detection of Brugada Syndrome Type 1 [4, 19]. The purpose of this chapter is to establish the theoretical and scientific background required to understand the proposed thesis work. Since this research combines cardiology, biomedical signal processing, ECG digitization, and deep learning, the literature review is organized into both clinical and technical sections.

The chapter begins by discussing Brugada Syndrome as an inherited arrhythmogenic disorder associated with sudden cardiac death [4]. It then explains the electrocardiographic basis of Brugada Syndrome, with specific emphasis on the Type 1 pattern, which is the main focus of this thesis. After that, the chapter reviews the challenges of ECG interpretation, the importance of right precordial leads, and additional ECG features that may support diagnosis. The chapter also discusses the role of signal processing and machine learning in ECG-based disease detection, including convolutional neural networks, recurrent neural networks, and attention mechanisms [27, 28, 29].

Finally, the chapter reviews the research gap addressed by this thesis. Most existing AI-based ECG studies rely on already digitized ECG datasets [30, 31, 33]. In contrast, this thesis begins from ECG records originally available in PDF format and develops a complete pipeline from digitization to deep learning classification. This makes the proposed work both clinically relevant and technically significant.

2.2 Clinical Background of Brugada Syndrome

Brugada Syndrome is an inherited cardiac electrical disorder associated with an increased risk of life-threatening ventricular arrhythmias and sudden cardiac death [4, 3, 19]. It is commonly classified as a cardiac channelopathy because it is often linked to abnormalities in ion channels responsible for cardiac action potential generation and propagation. The most frequently discussed genetic association is related to sodium channel dysfunction, particularly involving the cardiac sodium channel gene SCN5A [34, 35]. However, not all patients with Brugada Syndrome have an identifiable genetic mutation, which means that ECG interpretation remains a central component of diagnosis.

Unlike structural cardiac diseases, Brugada Syndrome often occurs in individuals without visible abnormalities in cardiac structure. This characteristic makes the syndrome particularly challenging because conventional imaging methods may not reveal the underlying risk. Instead, the disease manifests primarily through abnormal electrical activity, which can be observed through electrocardiographic patterns [26, 7]. These ECG patterns are especially important in the right precordial leads, mainly V1, V2, and V3 [7, 24].

The clinical relevance of Brugada Syndrome is high because some patients may remain asymptomatic until a serious arrhythmic event occurs. In some cases, sudden cardiac death may be the first manifestation of the disease [4, 19]. Therefore, early recognition of suspicious ECG patterns is important for clinical evaluation, risk stratification, and preventive decision-making [35, 36]. This thesis focuses specifically on the automated detection of the Type 1 Brugada pattern, also referred to as the Definitive class in the dataset.

2.3 Electrophysiological Basis of Brugada Syndrome

The electrophysiological mechanisms of Brugada Syndrome are complex and have been explained using different theories [3, 34]. Two major explanations are commonly discussed: the repolarization theory and the depolarization theory [3, 26]. These mechanisms are not necessarily mutually exclusive and may both contribute to the ECG abnormalities observed in Brugada Syndrome.

The repolarization theory suggests that Brugada Syndrome results from an imbalance between inward and outward ionic currents during the early phases of the cardiac action potential [3, 34]. A reduction in inward sodium current can increase transmural voltage gradients, particularly in the right ventricular outflow tract [34, 35]. This electrical heterogeneity may produce ST-segment elevation in the right precordial leads and create a substrate for ventricular arrhythmias [3].

The depolarization theory emphasizes delayed conduction in the right ventricular outflow tract [26, 34]. According to this view, conduction slowing or localized delay can produce abnormal QRS-ST morphology and contribute to the ECG pattern associated with Brugada Syndrome [26, 35]. This is particularly relevant because Brugada ECG features may overlap with conduction abnormalities such as right bundle branch block [7]. Differentiating true Brugada morphology from similar ECG patterns is therefore an important diagnostic challenge.

Both theories support the importance of analyzing the QRS complex, J-point, ST segment, and T wave [7, 24]. These regions of the ECG waveform are central to the detection of Type 1 Brugada morphology [7] and are therefore emphasized in the preprocessing and neural network design used in this thesis.

2.4 Standard ECG Fundamentals

The electrocardiogram is a non-invasive recording of the electrical activity of the heart [37, 38]. A standard 12-lead ECG provides different views of cardiac depolarization and repolarization by recording voltage differences from multiple electrode positions [37]. Each ECG lead represents electrical activity from a different anatomical perspective, allowing clinicians to detect rhythm disturbances, conduction abnormalities, ischemic changes, and inherited arrhythmia patterns.

A typical ECG waveform consists of several components [38, 37]. The P wave represents atrial depolarization, while the PR interval reflects conduction from the atria through the atrioventricular node to the ventricles. The QRS complex represents ventricular depolarization and is usually the most prominent component of the ECG [39]. The ST segment represents the early phase of ventricular repolarization, and the T wave represents later ventricular repolarization.

For Brugada Syndrome Type 1, the most clinically relevant region is the QRS-ST-T complex [7, 24]. The diagnostic morphology is observed around the terminal part of the QRS complex and the beginning of the ST segment. A coved ST-segment elevation followed by a negative T wave is characteristic of the Type 1 pattern [4, 26, 7]. Therefore, any automated system designed to detect Brugada Type 1 must preserve the morphology of this region during preprocessing and feature extraction [7].

2.5 Brugada ECG Pattern Classification

Brugada ECG patterns are commonly classified into different types based on their morphology [26, 3]. The most clinically important distinction is between Type 1 and non-Type 1 patterns [19, 35]. Type 1 is considered the diagnostic pattern,

while Type 2 and Type 3 patterns may be suspicious but are not definitive on their own.

The Type 1 pattern is characterized by coved ST-segment elevation, usually in the right precordial leads [4, 7]. This elevation is followed by a negative T wave [7]. The Type 2 pattern is often described as a saddleback pattern and may require further clinical evaluation or pharmacological testing to determine whether a true Type 1 pattern can be induced [26, 19]. Type 3 is generally less pronounced and has lower diagnostic specificity [26].

This thesis focuses specifically on Type 1 Brugada Syndrome [4, 19]. In the dataset and model implementation, this class is represented as *Definitive*. The opposing class is represented as *Non-BrS*. Therefore, the problem is formulated as a binary classification task, where the model learns to distinguish ECG windows with definitive Type 1 morphology from ECG windows without the definitive pattern.

2.6 Type 1 Brugada ECG Pattern

The Type 1 Brugada pattern is the central clinical target of this thesis [4, 19]. It is typically observed in leads V1, V2, and sometimes V3 [7, 26]. The pattern is characterized by a high take-off or J-point elevation, a coved ST-segment morphology, and a negative T wave [4, 7]. These features are not only visually important but also represent the morphological basis for automated ECG analysis.

Recent electrocardiographic consensus-based descriptions have refined the understanding of Type 1 Brugada morphology [7, 35]. In addition to ST-segment elevation, the shape and temporal evolution of the ST segment are important. The ST segment typically shows a progressive decline after the high take-off point, and this behavior helps differentiate Brugada Syndrome from other conditions such as incomplete right bundle branch block or athlete-related ECG patterns [7, 26].

For automated detection, these characteristics imply that the model should focus on the portion of the ECG signal following ventricular depolarization. This is why the preprocessing pipeline in this thesis extracts windows around the S-peak, including the region before and after the S wave. The post-S segment contains the ST segment and T wave, which are critical for detecting Brugada Type 1 morphology [7, 24].

2.7 Right Precordial Leads and Their Clinical Importance

The right precordial leads, especially V1, V2, and V3, are the most important leads for detecting Brugada Syndrome Type 1 [4, 26, 19]. These leads are positioned

over the right anterior chest and reflect electrical activity near the right ventricular outflow tract [3, 34]. Since Brugada Syndrome is strongly associated with abnormalities in this anatomical region, the right precordial leads are central to clinical ECG interpretation [7, 35].

In this thesis, the machine learning pipeline focuses on V1, V2, and V3. This decision is clinically motivated and technically consistent with the reference neural-network approach used as the basis for implementation [23]. The model receives these three leads as a multi-channel input, allowing it to learn both individual waveform morphology and cross-lead relationships. This is important because the appearance of ST-segment elevation may vary across V1, V2, and V3.

The use of multiple right precordial leads is also advantageous because it preserves spatial information [23]. A single-lead model may detect local waveform abnormalities, but it cannot fully capture how morphology changes across adjacent precordial leads. By using V1–V3 as a three-channel input, the neural network can learn inter-lead gradients and relationships that may be relevant to Brugada Type 1 detection.

2.8 Differential Diagnosis and Similar ECG Patterns

One of the major challenges in Brugada Syndrome diagnosis is differentiating true Type 1 Brugada morphology from other ECG patterns that may appear similar [26, 19, 35]. Conditions such as right bundle branch block, incomplete right bundle branch block, early repolarization, arrhythmogenic right ventricular dysplasia, and Brugada phenocopies can produce ECG abnormalities that resemble Brugada patterns [7, 26].

Right bundle branch block is particularly important because it may show terminal positive deflections in the right precordial leads [7]. However, the morphology of the ST segment and the QRS complex can help distinguish it from Brugada Syndrome [7, 24]. In Brugada Syndrome, the r' wave may appear broader and more rounded, and the ST segment may show a characteristic coved decline. In contrast, incomplete right bundle branch block often has a sharper r' morphology [7].

The distinction between Brugada Syndrome and similar ECG patterns is clinically important because misclassification may lead to inappropriate risk assessment [19, 35]. For machine learning, this means that the model must learn subtle morphological differences rather than relying only on simple amplitude thresholds. This supports the use of deep learning models capable of extracting complex patterns from ECG signals [30, 31, 33].

2.9 Advanced Electrocardiographic Features in Brugada Syndrome

Recent clinical literature has described additional ECG features that may improve the recognition of Brugada patterns [7]. These include details related to the high take-off of the QRS-ST segment, ST-segment slope, r' wave morphology, QRS duration mismatch, and quantitative angle measurements [7]. Such features help clinicians differentiate Brugada patterns from other ECG abnormalities [7, 24].

For example, the morphology of the r' wave in V1 and V2 can provide useful information [7]. In Brugada Syndrome, the r' wave is often broad, rounded, and associated with slow descent [7]. This differs from the sharper r' wave typically seen in incomplete right bundle branch block [7]. Quantitative measurements such as alpha and beta angles have also been proposed to assist in differentiating Brugada patterns from other conditions [7].

These advanced features are relevant to this thesis because they demonstrate that Brugada detection is not based only on one simple measurement [7, 24]. Instead, it requires analysis of waveform shape, timing, amplitude, and inter-lead morphology. Deep learning is suitable for this type of problem because convolutional and recurrent layers can learn complex signal representations without requiring all features to be manually engineered [27, 28, 30].

2.10 Inferior Lead Findings in Brugada Syndrome

Although Brugada Syndrome is traditionally associated with right precordial leads, some studies have suggested that additional information may be present in other leads [4, 7]. One important finding is the presence of ST-segment depression in inferior leads such as II, III, and aVF in some Type 1 Brugada cases [24]. This observation suggests that Brugada-related electrical abnormalities may not be limited only to V1–V3 [24].

A study analyzing patients with Type 1 Brugada pattern reported that ST-segment depression in the inferior leads was present in a significant proportion of cases [24]. This finding may help identify cases where the classical right precordial Brugada pattern is not immediately obvious [24]. It also suggests that future AI models may benefit from incorporating additional leads beyond V1–V3 [24].

In this thesis, the model focuses on V1–V3 to remain aligned with the primary diagnostic leads and the implemented reference architecture [23]. However, the inferior lead findings are important for future work. A future extension of this research could include leads II, III, and aVF together with V1–V3 to evaluate whether additional lead information improves classification performance.

2.11 Pharmacological Provocation Testing

In some patients, the Type 1 Brugada pattern is not visible during a baseline ECG [26, 19]. In such cases, pharmacological provocation testing may be used to unmask the diagnostic pattern [26, 35]. Sodium channel blockers, such as ajmaline, may reveal concealed Brugada morphology by reducing sodium current and accentuating the underlying electrical abnormality [3, 34].

Although provocation testing can be clinically useful, it requires careful medical supervision because it may induce arrhythmias or other adverse events [19, 35]. This makes it unsuitable as a simple screening approach in all settings. Therefore, non-invasive and automated methods for detecting hidden or subtle Brugada-related patterns from baseline ECGs are valuable [30, 31].

The dataset used in this thesis includes baseline ECG recordings and AJM or provocation related recordings. This reflects the clinical reality of Brugada Syndrome evaluation. However, the long-term motivation of this work is to support non-invasive detection using digitized ECG signals, reducing dependence on risky or resource-intensive diagnostic procedures.

2.12 Signal Processing in ECG Analysis

ECG signals are biomedical time-series signals that often require preprocessing before analysis [37, 38]. Raw ECG recordings may contain baseline wander, powerline interference, motion artifacts, muscle noise, and digitization-related distortions [38, 37]. These sources of noise can affect both manual interpretation and automated classification [40].

Signal processing is therefore a critical step in ECG-based machine learning [37, 38]. Typical preprocessing steps include interpolation, filtering, baseline correction, normalization, segmentation, and quality control [40, 41]. In this thesis, digitized XLSX signals are interpolated to a standard sampling rate and cleaned before window extraction. This ensures that all signals have a consistent temporal structure suitable for neural network training.

Segmentation is also important [39, 41]. Instead of using long ECG traces directly, the proposed method extracts fixed-length windows around the S-peak. This approach focuses the model on the clinically relevant QRS-ST-T region while reducing irrelevant signal portions [7, 24]. Since Brugada Type 1 morphology is mainly expressed after the S wave, S-peak-centered windows are clinically appropriate [7].

2.13 Artificial Intelligence in ECG Diagnosis

Artificial intelligence has been increasingly applied to ECG interpretation [30, 31, 33]. Machine learning models can identify patterns that may be difficult for humans to detect, especially when features are subtle, distributed, or non-linear [42, 30]. Traditional machine learning methods often require handcrafted features, while deep learning methods can learn features directly from the signal [42, 27].

Deep learning has shown strong performance in tasks such as arrhythmia detection, atrial fibrillation classification, myocardial infarction detection, and inherited cardiac disorder screening [30, 31, 33]. In ECG analysis, neural networks are particularly useful because ECG signals contain both local morphology and temporal dependencies [27, 28]. For this reason, architectures combining convolutional and recurrent components are commonly used [43, 44, 45].

In the context of Brugada Syndrome Type 1, AI may help detect subtle waveform characteristics around the QRS-ST-T region [23]. It may also help reduce subjectivity in ECG interpretation. However, AI systems require carefully prepared datasets, appropriate preprocessing, reliable labels, and clinically meaningful evaluation metrics [30, 31, 25, 32].

2.14 Convolutional Neural Networks for ECG Signals

Convolutional neural networks are commonly used for biomedical signal classification because they can extract local patterns from time-series data [27, 44, 45]. In one-dimensional ECG signals, convolutional filters slide along the time axis and learn morphological features such as sharp QRS complexes, ST-segment shapes, and T-wave patterns [44, 43].

In this thesis, the model uses one-dimensional convolutional layers. The convolutional blocks learn local ECG waveform features from the V1, V2, and V3 input channels [27, 44]. Early convolutional layers may capture simple waveform edges and slopes, while deeper convolutional layers may capture more complex Brugada-related morphology [27].

The use of multiple convolutional blocks also reduces the need for manually defining ECG features [27, 42]. Instead of explicitly measuring ST elevation, QRS duration, or T-wave inversion, the model learns signal representations from labeled examples [42, 30]. This is useful when the dataset contains variability due to patient differences, digitization quality, and recording conditions.

2.15 Recurrent Neural Networks and BiLSTM Layers

Although convolutional layers are effective for local feature extraction, ECG signals also contain temporal dependencies [27, 28]. The interpretation of a waveform region often depends on what occurs before and after it. For example, ST-segment morphology must be interpreted in relation to the QRS complex and T wave. Recurrent neural networks are designed to model such sequential relationships [28].

Long Short-Term Memory networks are a type of recurrent neural network that can learn temporal dependencies over longer sequences [28]. A bidirectional LSTM processes the sequence in both forward and backward directions [46]. This allows the model to use information from both earlier and later parts of the ECG window when forming its representation [46].

In this thesis, two bidirectional LSTM layers are used after the convolutional feature extractor. This design allows the model to combine local morphology extracted by convolutional filters with temporal context learned by recurrent layers [27, 28]. This combination is suitable for Brugada Type 1 detection because the diagnostic morphology is not limited to a single point but is distributed across the QRS-ST-T complex[7, 24].

2.16 Attention Mechanisms in ECG Classification

Attention mechanisms allow neural networks to assign different importance weights to different parts of an input sequence [29, 47]. In ECG classification, attention can help identify which time regions contribute most strongly to the model's prediction [43, 30]. This is valuable because medical AI systems should ideally provide some level of interpretability [31].

In Brugada Syndrome Type 1 detection, attention is expected to focus on clinically relevant regions such as the S-peak, J-point, ST segment, and T wave [7, 24]. If the attention weights highlight these regions, the model's decision becomes more interpretable. Attention maps can therefore support clinical review by showing whether the model is focusing on plausible ECG regions [29].

The model implemented in this thesis includes a custom additive attention layer after the bidirectional LSTM layers [29]. This layer computes attention weights over the temporal sequence and produces a context vector used for final classification [29, 47]. The evaluation stage generates attention maps over ECG windows, allowing visual analysis of model focus across the input signal.

2.17 MeMeA 2025 Brugada Classification Approach

The neural network implementation in this thesis was inspired by the MeMeA 2025 Brugada classification approach[23]. The reference methodology combines convolutional layers, bidirectional LSTM layers, and an attention mechanism for ECG-based Brugada classification [23]. The architecture is designed to capture local waveform morphology, temporal sequence information, and relevant signal regions [23].

The original MeMeA 2025 framework is associated with a three-class Brugada classification problem, including Definitive, Borderline, and Non-Brugada cases [23]. In this thesis, the approach is adapted to a binary classification problem because the main research focus is the detection of Brugada Syndrome Type 1, represented by the Definitive class. The output of the implemented model therefore distinguishes between Non-BrS and Definitive / Brugada Type 1.

This adaptation is clinically meaningful because Type 1 is the diagnostic Brugada ECG pattern [4, 19]. The use of V1–V3 leads, S-peak-centered windows, convolutional feature extraction, recurrent temporal modeling, and attention-based interpretation provides a strong foundation for automated Brugada Type 1 detection [23].

2.18 Comparison of Related Studies

Table 2.1 summarizes the main literature areas relevant to this thesis. The reviewed studies include clinical ECG studies, advanced ECG morphology papers, and artificial intelligence-based Brugada detection approaches[4, 7, 24, 23].

Table 2.1: Comparison of related studies and relevance to this thesis

Study / Area	Main Focus	Method	Relevance to This Thesis
Brugada clinical ECG literature	Type 1 diagnostic morphology	Expert ECG interpretation	Defines the clinical target: Type 1 / Definitive pattern
Advanced ECG features in Brugada Syndrome	QRS-ST morphology, r' wave, differential diagnosis	Morphological ECG analysis	Supports focus on waveform morphology and V1–V3 leads
Inferior lead ST depression study	Additional ECG markers outside V1–V3	Clinical ECG analysis	Suggests future extension using II, III, and aVF leads
MeMeA 2025 Brugada approach	AI-based Brugada classification	CNN, BiLSTM, Attention	Provides reference architecture for neural network implementation
This thesis	PDF ECG digitization and binary Type 1 detection	ECGD, preprocessing, CNN-BiLSTM-Attention	Provides end-to-end pipeline from PDF ECG to AI prediction

The comparison shows that existing clinical studies provide strong knowledge about Brugada morphology, while AI-based studies demonstrate the feasibility of automated classification [7, 24, 23, 30, 31]. However, many existing approaches assume that ECG signals are already available in digital form [30, 31, 33]. This thesis contributes by addressing the practical challenge of converting PDF ECG records into numerical signals before applying machine learning.

2.19 Research Gap

The literature shows that Brugada Syndrome Type 1 is clinically important and that ECG morphology plays a central role in diagnosis [4, 19, 7]. It also shows that artificial intelligence can support ECG classification by learning complex waveform patterns [30, 31, 33]. However, several gaps remain.

First, many AI-based ECG studies rely on ready-to-use digital ECG datasets [30, 31, 33]. In real clinical environments, ECG records may exist as PDF reports, scanned images, or printed documents. These formats cannot be directly used for signal processing or neural network training. Therefore, there is a need for workflows that convert ECG records from PDF format into structured digital

signals.

Second, Brugada Type 1 detection requires careful preservation of QRS-ST-T morphology [7, 24]. Preprocessing steps such as normalization, filtering, and segmentation must be designed so that clinically relevant features are not destroyed. This is especially important because ST-segment elevation is an amplitude-sensitive diagnostic feature [4, 7].

Third, class imbalance is a common issue in medical datasets [48, 32]. In this thesis, the cleaned dataset contains more Definitive samples than Non-BrS samples. Without appropriate handling, a model may become biased toward the majority class. This creates the need for class-balancing strategies and careful evaluation using precision, recall, F1-score, and confusion matrix analysis [32, 48].

Fourth, interpretability remains a key challenge in medical AI [30, 31]. Deep learning models can achieve good performance but may be difficult to explain. The use of attention maps provides one way to inspect which ECG regions contribute to model predictions [29]. However, attention behavior must still be analyzed carefully to ensure clinical plausibility.

This thesis addresses these gaps by developing an end-to-end pipeline for Brugada Syndrome Type 1 detection. The pipeline includes ECG digitization from PDF records, dataset cleaning, signal preprocessing, S-peak-centered window extraction, CNN-BiLSTM-Attention model implementation, threshold optimization, and evaluation with both quantitative metrics and visual interpretation.

2.20 Chapter Summary

This chapter reviewed the clinical and technical literature relevant to the automated detection of Brugada Syndrome Type 1. It discussed the clinical background of Brugada Syndrome, the importance of Type 1 ECG morphology, the role of the right precordial leads, and the challenges of differentiating Brugada patterns from similar ECG abnormalities .

The chapter also reviewed the role of ECG signal processing and artificial intelligence in automated cardiac diagnosis. Convolutional neural networks, bidirectional LSTM layers, and attention mechanisms were discussed as key components of the model used in this thesis. The literature review showed that while existing studies provide important clinical and technical foundations, there remains a need for a complete pipeline that begins from PDF ECG records and produces machine-learning-based Brugada Type 1 predictions.

The next chapter presents the ECG digitization and dataset construction process. It explains how ECG records originally provided in PDF format were converted into XLSX numerical time-series signals and organized into a cleaned dataset suitable for neural network preprocessing and training.

Chapter 3

ECG Digitization and Dataset Construction

3.1 Introduction

In this chapter, you will find the full procedure used to digitize ECG readings taken in the form of PDF documents. In my thesis, ECG digitization is one of the key stages of work since the initial information was not given in the form of digital signals. The ECG readings were given in the form of analog PDF images that could be easily interpreted by specialists. However, this kind of ECG data cannot be analyzed both by neural networks and through signal processing techniques [37, 38]. Therefore, prior to creating a machine learning model, the analog signals had to be converted to time-series digital data.

The process of digitization acts as a link between clinical ECG recording and the analysis process. In most cases, the ECG signals are recorded in the form of scanned images, printed records, and PDF documents instead of digital data. While such data is good for inspection by the naked eye, they cannot be subjected to automation due to the fact that the signal is contained within the document as an image and not in numeric values with respect to time [37]. This therefore led to the initial focus of this thesis on extracting the ECG signal from the given PDF documents.

In this chapter, a comprehensive description is provided concerning the process of full digitization, which entails discussion regarding the origin of ECG data, the role of ECGD program, the process of analog to digital conversion, scaling, building of an XLSX dataset, and verification of the same. In addition, the obstacles faced during digitization include grid noise, waveform alteration, scaling problems, loss of data and file naming inconsistencies. Through provision of this detailed analysis, it is clear that the dataset used in the machine learning process was not sourced

from an existing digital library.

The resulting digitalized database contains 311 files in the format XLSX which are digitalized from the ECGs pertaining to different patients or case numbers. The digitized files contain baseline ECGs, AJM/provocation ECGs, and some other unknown files. The database serves as the basis for further processes such as the preprocessing stage and classification through a neural network. Hence, the accuracy of digitalization will affect the accuracy of the Brugada Syndrome Type 1 detection system.

3.2 Need for ECG Digitization

The necessity to digitize the ECG signal stems from the requirement of the learning algorithm to have numerical data for analysis [37, 38]. The neural network can't learn anything from the image in PDF format unless the image passes through a certain model designed for images. But in the thesis, the goal was to learn the ECG signals as biomedical time series signals. Hence, the wave forms in the ECG had to be extracted in numeric form [37].

The ECGs supplied for this thesis were originally in the form of PDFs. These PDFs had the ECG signals in the form of waves drawn on standard ECG grid paper. From a medical perspective, this is a good approach as doctors would analyze the wave,visually by determining characteristics like ST segment elevation, QRS wave morphology, and T wave configuration [7]. Nevertheless, from a computing perspective, these PDFs do not have actual time-voltage values associated with them [37]. They are represented in the form of a graph, which means digitization is required.

Digitization was crucial since the thesis concentrates on Type 1 Brugada syndrome, for which morphological aspects of the ECG carry clinical significance [4, 19]. Type 1 Brugada syndrome is associated with abnormalities predominantly in the right precordial leads, namely V1-V3 leads [26, 7]. The abnormalities manifest themselves in the form of coved-type ST segment elevation, along with T wave inversion [4, 7]. In case the digitization process is done incorrectly, the delicate features might not be captured by the system, negatively affecting its efficiency.

Another reason for which digitization becomes a necessity is the fact that medical data in the real world can be inconsistent, heterogeneous, and presented in varying formats. In most machine learning experiments, data that is already digitized from ECG recordings is used [30, 31, 33]. However, in clinical settings, ECG recordings are generally available only in PDF format as reports. In digitizing PDF ECG data to XLSX numerical data, this thesis tackles an existing problem in the processing of biomedical data.

3.3 Analog ECG, Digital ECG, and ADC Concept

The electrocardiogram (ECG) signal is basically a continuous analog signal obtained from the functioning of the heart [37, 38]. It represents the electric phenomena in which there is the depolarization and repolarization of the tissues [38]. In the conventional ECG reading, this analog signal is displayed as a continuous curve on a piece of paper or screen. If the ECG reading is converted to PDF format, then although the curve looks continuous, the values are not available directly.

On the contrary, a digital signal for ECG is also a waveform that consists of various discrete numbers [37]. These discrete numbers denote voltages at a certain time point. Digital data facilitates further processing, filtering, segmentation, and use as input for machine learning applications [37, 41]. The transition from analog to digital format bears many similarities to ADC. In the latter case, a continuous signal is also changed into digital data via sampling and quantization.

However, in relation to this thesis, the ECG has not been recorded by a direct connection to an electronic ADC device. The ECG waveform was available either in a printed form or as a PDF file format. The digitization process will then be seen as an attempt to reconstruct a digital signal from its graphical depiction. The ECGD software will recognize the ECG waveform within the PDF image, as well as assign the ECG waveform's position in the grid in terms of time and voltage levels.

ADC theory is relevant in describing this phenomenon because the digitized ECG consists of samples as a regular digital recording of an ECG would. In the former, time is measured on the X-axis while the amplitude is measured on the Y-axis. It is the sampling rate that determines how many points are taken along the time axis, and the quantization is what determines the precision of representation of the amplitude values. Thus, any deviation in the sampling rate and/or amplitude could affect the signal quality [37].

3.4 Source ECG Data and Clinical Format

The original ECG data that has been used in the present thesis consists of ECGs in the form of PDF files that contain clinical reports of ECG readings. In fact, PDF files were digitalized representation of analog ECGs. An ECG contained several leads, which corresponded to the 12-lead ECG. The 12-lead ECG shows the electrical activity of the heart at different angles and serves as a means of diagnosing rhythm problems, conduction problems, and repolarization problems [37, 38].

The diagnosis of Brugada Syndrome Type 1 requires focus on the right precordial

leads [4, 26, 19]. The leads V1, V2, and V3 are positioned over the right anterior chest region, and thus become clinically relevant when studying ST-segment variations associated with Brugada syndrome [7, 35]. The Type 1 Brugada electrocardiogram shows an elevation of the ST segment in the form of a cove and an inverted T wave [4, 7]. Consequently, particular emphasis was placed on these leads in data set formation and preprocessing stages.

There were variations in terms of the quality of recording, clarity of the image, visibility of the grid, and thickness of waveforms in some of the ECG images in PDF format. Variations of this nature often occur in clinical datasets that are used in actual practice. There are ECGs that could be clear and easier to digitize, whereas others could have noise or overlapping of grid or low resolution. Despite making the process of digitizing difficult, it made the data more realistic.

In addition, the database contained various types of ECGs like baseline ECGs and AJM or provocation ECGs [26, 19]. A baseline ECG is an ECG taken without any pharmacological stimulus whereas AJM ECG refers to the ajmaline provocation test. Ajmaline might be administered during the evaluation of Brugada Syndrome to detect concealed type 1 ECG patterns [35, 34]. Both these ECG types being present in the database provide valuable insights into the process of Brugada ECG patterns appearance.

3.5 ECGD Software and Digitization Environment

Conversion of ECG waveforms into digital signals was done through the use of ECGD software. ECGD was used to obtain ECG traces that were contained within PDF graphical representations of the data and transform them into numeric signal values. ECGD software played an important role in this thesis as it allowed transforming unstructured data into structured signals.

The function of the ECGD software involves recognizing the pattern of the ECG graph and encoding the graph coordinates as numerical data. In a PDF ECG graph, the graph pattern is shown as pixels or graphical lines. The program recognizes where the graph sits relative to the ECG grid and decodes the signal based on a known time scale and voltage scale for that particular graph [37]. To do so, the program needs to recognize the grid distance, determine the horizontal time scale, and calculate the vertical voltage scale.

Digitization of the ECG signal entailed the careful manipulation of each individual ECG file. The quality of the signal that would be extracted was dependent on the quality of the ECG itself, proper calibration of the grid and the accuracy of the waveform's trace. If the grid was calibrated incorrectly, there could be errors in the time and voltage scale of the extracted signal. Likewise, any inaccuracies

in the waveform's trace could alter the shape of features such as the ST segment elevation or the QRS wave.

The output of the ECGD module is in the XLSX format. XLSX was chosen because it enables the saving of the extracted numbers as tabular data. Moreover, the XLSX format allows us to easily inspect the file visually, as well as to read it in a Python program where we could do preprocessing and analysis. In our project, XLSX files obtained from ECGD served as the main datasets.

3.6 PDF ECG to XLSX Workflow

The entire process of digitizing starts from the original PDF files of the ECG records and ends with the validated XLSX files holding the numeric values for the ECG signals. The described process is one of the greatest contributions that have been made in the thesis. The complete workflow is shown in Figure 3.1.

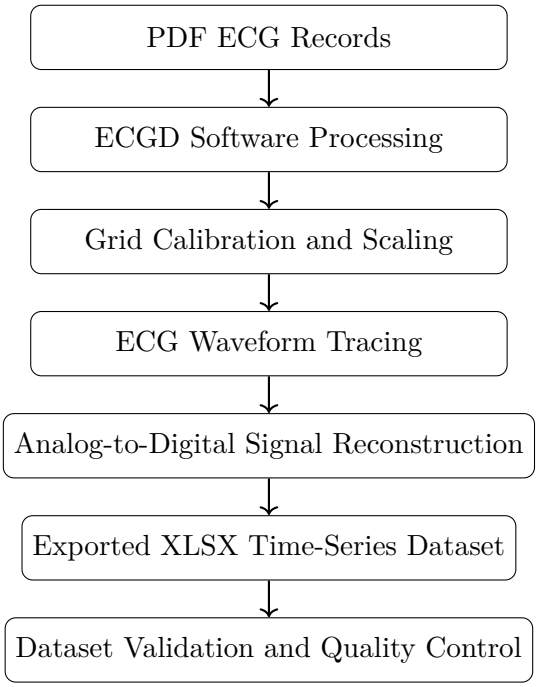

Figure 3.1: ECG digitization workflow from PDF records to XLSX dataset

Step one in the workflow is importing the PDF ECG reading into the ECGD application. Upon successful importation, calibration of the grid is done so that the program can decipher the time and voltage scale from the graph [37]. This is because the time scale is measured using horizontal grid spacing whereas the voltage is measured using vertical grid spacing [38]. After the calibration of the

grid, the ECG waveform is digitized.

Post-waveform plotting, the data is re-created digitally in a form of time series. This step involves the conversion process much in a way that ADC does since the continuous waveform plot is converted into numeric points [49]. The obtained values are stored in XLSX files. The data is then verified for correctness and used in the subsequent preprocessing step.

The procedure guarantees that the digitized dataset will retain all the fundamental characteristics of the ECG signal. In addition, the process offers traceability such that the digitized data files can be traced back to their original PDF sources. This is important in terms of quality assurance and providing an understanding of the data set development process.

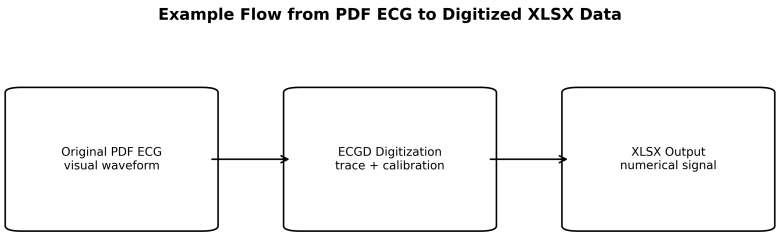

Figure 3.2: Example flow from PDF ECG to digitized XLSX data

3.7 Signal Extraction and Scaling

The procedure whereby the ECG wave is extracted from the PDF file is termed signal extraction. The reliability of the procedure depends mainly on scaling, which is accurate only when properly done. For instance, an ECG normally has time on the horizontal axis while the vertical axis contains the voltages [37, 38]. The standard scale of the ECG paper may, for example, involve 25 mm/s and 10 mm/mV [37]. However, the exact scale has to be verified from the ECG sheet.

The scaling procedure starts with determining or measuring the grid parameters. Once the grid has been determined, then one can calculate the number of pixels per unit time interval or unit voltage. In this regard, the distance between each line along the horizontal grid is used to construct the time scale, and the distance between lines on the vertical grid is used to construct the signal voltage. Failure to accurately identify the grid could result in distortion of the signal [37].

Waveform tracing is another vital process in signal extraction. The ECG waveform may have overlapped with various graphical components, including gridlines and text markings. It is crucial for the computer program to determine which one among the graphical data is the true waveform. At times, human

intervention may still be necessary to make sure that the signal extraction follows the true ECG waveform. This is especially critical in Brugada Syndrome Type 1 because its features are difficult to spot [7, 4].

Following scaling and tracing, the extracted waveform is then sampled and turned into numbers that form the digital signal [37, 38]. The signal sample is actually the amplitude value of the signal at that particular time. Finally, the digital signal can be stored using the XLSX file format. With the digitized version of the ECG, further analyses can now be done.

3.8 Dataset Construction in XLSX Format

Following the process of digitization, the ECG signals were stored in XLSX file formats. This format is suitable for saving numeric ECG data in a table. The contents of each file are an ECG signal or an ECG page depending on how the original record in PDF format was organized. These files contain data that can be used in Python.

The creation of the XLSX dataset was done by sorting out the digitized records using patient/case identification, recording type, and source of ECG. There are baseline ECG recordings and AJM/provocation related ECG recordings in the XLSX dataset. Due to the reason that there may be several pages for each ECG report, each clinical ECG record can be represented by multiple XLSX records. This is the reason behind having more XLSX records than ECG records.

The use of the XLSX format proved beneficial in the course of the implementation process since it permitted manual inspection of the signals' values. It is significant for a digitizing process because errors might arise when extracting the waveforms from the video. Manual inspection of the files in XLSX format helped check the reasonability of the values obtained, the continuity of the signal, and the presence of usable information.

The final dataset formed the basis for further work in the thesis. After obtaining the data as numeric ECG signals, it was possible to apply the usual techniques of signal processing on the obtained data [37, 38]. This dataset provided the possibility of performing such actions as filtering, normalizing, segmenting, and classifying by a neural network in future steps of research [37, 41]. Thus, the construction of an XLSX dataset became an important step in the research method.

3.9 Dataset Summary

The final digital dataset is made up of 311 XLSX files that were derived from the initial PDF file for the ECG data. This means that the above files constitute the digitized version of the ECG signal data. The dataset contains about 27 cases and

nearly 90 ECGs because sometimes an ECG document may contain multiple pages. The reason for this is that there are some AJM/provocation ECG recordings too.

Table 3.1: Summary of digitized ECG dataset

Parameter	**Value**
Total digitized XLSX files	311
Patient / case identifiers	27
Approximate unique ECG records	90
Baseline ECG XLSX files	167
AJM / provocation-related XLSX files	143
Other / unclear files	1
Original data format	PDF ECG records
Output data format	XLSX numerical time-series
Main clinical focus	Brugada Syndrome Type 1
Important leads	V1, V2, V3

Table 3.1 It provides an overview of the general structure of the database. The presence of 311 XLSX files implies that numerous signal data have been created based on the initial PDF files. The number of patient ID numbers suggests that the database consists of more than one clinical case. The total number of ECG cases can be considered smaller than the total number of XLSX files since multiple ECG files have been split into different parts or files.

The distinction between the baseline and ajmaline/provocation ECGs is pertinent to Brugada syndrome [26, 19]. Baseline ECGs are those which have never been exposed to any drugs, whereas ajmaline/provocation ECGs are those in connection with the ajmaline test and can reveal a concealed Type 1 Brugada pattern [34, 35]. There are 167 baseline and 143 AJM/provocation ECGs in the existing dataset, including 1 unknown case.

3.9.1 Combined Raw Digitized Dataset

The original digitized data set for use in the thesis comprised several different data sets. One of them consisted of 311 digitized XLSX files based on ECG data supplied in PDF form. In order to add more digitized files to the data set and thus enhance model generalization, the author added ECG files provided by co-workers. They consisted of the Waqas khan and Muhammad Hammad Rauf data sets.

The number of digitized files within the Waqas combined dataset was 414 XLSX files, whereas the total number of digitized files within the Hammad dataset was 316 XLSX files. In terms of the final digitized dataset, the number of XLSX ECG

files was 1041.

Table 3.2: Combined raw digitized ECG dataset

Dataset Source	**Digitized XLSX Files**
Author's digitized dataset	311
Waqas combined dataset	414
Hammad dataset	316
Total digitized ECG files	**1041**

Table 3.2 This section will summarize the aggregate raw digitized database. The need for more digitized files was necessary due to the fact that deep learning models need an adequate amount of data to recognize patterns. Nonetheless, the aggregate raw dataset could not be employed directly to train the model as there were some digitized files which had invalid or inconsistent labels.

3.9.2 Dataset Cleaning and Label Mapping

Following the completion of the creation of the combined raw data set, the subsequent stage involved cleaning of the data set and mapping of the labels. The primary aim at this stage was to determine whether the digitized ECG data sets were labeled and classify them appropriately.

Clinical labels data were kept in a report file where case names and Brugada Type 1 label were listed. In the dataset cleaning process, labels data were used to match each XLSX file with its respective class. Those which were identified with Brugada Type 1 label were put under the *Definitive* folder, and those that did not belong to Brugada Type 1 went under the *Non-BrS* folder.

Cleaning of the dataset became necessary owing to the presence of files having different formats of contributors' folders and naming conventions, along with complicated paths and page numbers in some files. For this reason, the task required uniformity in file names, identifying the page numbers of the documents, and detecting the match between base case names.

A total of 1041 XLSX files have been cleaned through the process. Out of these files, 784 files were able to map themselves to valid labels to form the cleaned dataset. A total of 257 files had to be removed since they were either unlabelled or did not align with the label report.

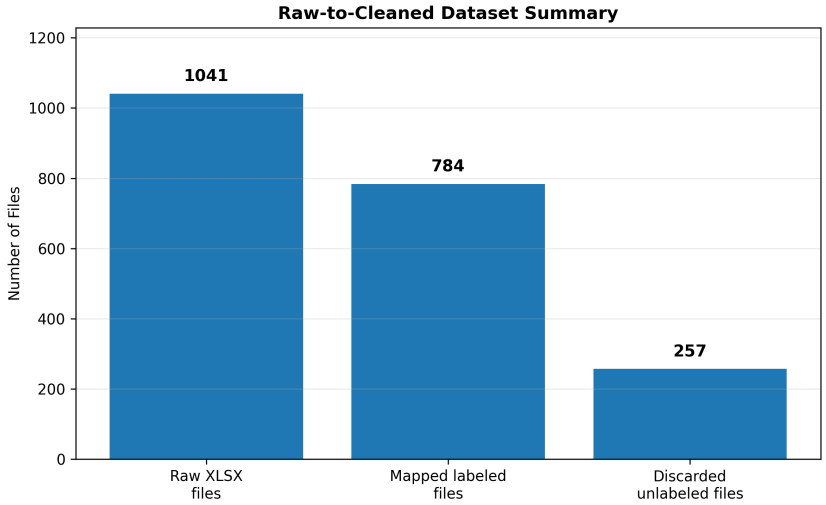

Figure 3.3: Raw to cleaned dataet summary

Table 3.3: Raw to cleaned dataset summary

Dataset Stage	Count
Raw XLSX files evaluated	1041
Successfully mapped labeled files	784
Discarded unlabeled files	257
Definitive / Brugada Type 1 files	610
Non-BrS files	174

Table 3.3 This demonstrates the process of transformation from the initial digital dataset to the final clean dataset. In the clean dataset, there were 610 files categorized as Definitive and 174 files categorized as Non-BrS. From the class distribution above, it is evident that there was class imbalance, since there were more Brugada Type 1 files compared to Non-BrS files [32, 48].

3.9.3 Cleaned Dataset Structure

The final cleansed data set was divided into two major directories named *Definitive* and *Non-BrS*. The *Definitive* directory comprises ECGs related to the Type 1 Brugada syndrome, whereas the *Non-BrS* directory includes ECGs that do not match the criteria for the definitive Type 1 Brugada syndrome. The two-fold classification was adopted for supervised machine learning.

The cleaned dataset structure can be represented as follows:

```
cleaned_dataset/
|-- Definitive/
|   |-- ECG_file_1.xlsx
|   |-- ECG_file_2.xlsx
|   |-- ...
|
|-- Non-BrS/
    |-- ECG_file_1.xlsx
    |-- ECG_file_2.xlsx
    |-- ...
```

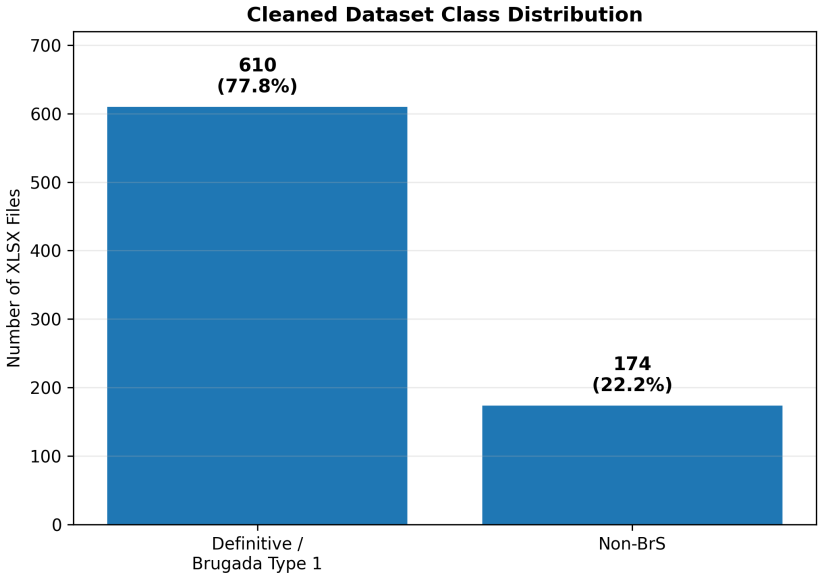

Figure 3.4: Cleaned dataset class distribution

This structure enabled the preprocessing script to automatically classify the folders according to the folder names, assigning label 1 for the *Definitive* folder and label 0 for the *Non-BrS* folder. Such automatic assignment of labels minimized potential human mistakes when importing the data for model training.

However, this clean data set did not form the machine learning sample set. It rather formed the input file to the pre-processing step, where multiple heartbeat centered windows were extracted from each individual ECG file, giving us more ECG windows to train our neural network.

3.9.4 Dataset Consistency Report

A process of evaluating the consistency of the dataset was carried out to ensure the clinical label file is consistent with the ECG files that were in the folders. The reason for doing so is that real-world datasets are known to have inconsistencies, extra files, or missing files [42].

215 valid labeled instances have been reported in the clinical label report for this particular data set. Out of these, there were 165 different base cases in the cleaned data set. There were 50 labeled instances missing from the folders of the data set. Besides, there were 61 additional data sets that were missing from the label report.

Table 3.4: Dataset consistency report

Item	Count
Valid labeled instances in clinical report	215
Distinct base cases present in cleaned dataset	165
Labeled cases missing from dataset folders	50
Extra datasets without label report	61

Table 3.4 It brings into focus the practical problems related to data preparation for the analysis. The lack of labeled samples was problematic since the ECG file for those could not be found. Any extra samples with no labels were removed because labeled samples are needed for supervised learning [42].

The purpose of this summary is to provide information about the data set without including long tables for each particular patient in the thesis chapter. The main goal of this summary is to provide an insight into important aspects of the data set rather than all patients involved in the research.

3.10 Digitization Challenges

There were some technical difficulties associated with the digitizing process. First of all, there was a problem of grid interference. Typically, an ECG report is recorded on grid paper with grid lines running vertically and horizontally [37, 38]. It helps measure the data on the chart. When digitizing such records, the grid lines may create interference while trying to separate the waveform from the rest of the background. In case their intensity/color coincides, the accuracy suffers.

A further issue that was encountered was inconsistency in the quality of the PDFs. While some ECG reports contained more clearly defined waveforms, others were low-resolution, resulting in poor tracing of the waveforms. Poor image quality

results in inconsistencies in the waveform extraction process, leading to improper waveform tracing or even loss of waveform morphology altogether. This is especially significant considering that Brugada Syndrome Type 1 has subtle diagnostic features [4, 7].

Mismatches in scaling were another possible source of errors. Digitization requires accurate mapping of pixels to physical quantities. Incorrect scaling of time or voltage would render the obtained signal inconsistent with the actual ECG being analyzed. Clinically meaningful parameters such as QRS width and height of ST elevation can be adversely affected by incorrect scaling [7, 37]. Scaling should have thus been performed in conjunction with digitization.

Moreover, certain ECG recordings consisted of more than one page, or even repetitions. This made data organization difficult when creating the database as the files needed to be labeled, organized, and checked to make sure there were no duplications of pages, missing pages, mislabeled files, or different types of recordings. It shows that making a dataset out of actual clinical PDF files is a complex process involving not only software but also engineering.

Table 3.5: Digitization challenges and their possible impact

Challenge	**Description**	**Possible Impact**
Grid interference	ECG waveform overlaps with grid lines	Incorrect waveform tracing
Low image quality	PDF resolution or contrast may vary	Loss of signal detail
Scaling mismatch	Time/voltage calibration may be inaccurate	Distorted ECG intervals or amplitudes
Multi-page ECG reports	One ECG record may produce several files	Dataset organization complexity
Unclear filenames	Some files may not indicate recording type	Difficulty in classification and validation
Signal discontinuity	Extracted waveform may contain gaps	Reduced preprocessing quality

Table 3.5 identifies some of the digitization issues that were encountered while developing the dataset. The digitization issues were sorted out by doing inspections, organizing files, and validating the data before embarking on machine learning.

3.11 Data Validation and Quality Control

Once the digitalization was complete, the data set needed to be validated so as to determine whether the files obtained had been organized well enough. Validation is a crucial step whenever you want to perform machine learning tasks [42]. In our case, it was even more necessary since the data set originated from analog and PDF files.

Validation comprised the examination of file readability, verification that the signals consisted of numerical values, and evaluation of the waveforms to ensure consistency with ECG characteristics [37, 38]. Careful consideration was given to files lacking numerical data, uninterpretable formatting, or unclear content. The goal was to validate the presence of trustworthy digitized signals prior to further processing and classification.

An equally vital aspect of quality control was checking for consistency between ECG files available and the expected labels or classes of recording. It is quite common in clinical data that there are inconsistencies between records and the availability of ECGs [42]. There could be missing records, but other records would have no labels at all. This problem was dealt with through summarization of the files available into clear categories.

Data quality control also entailed ensuring that the data structure was correct after extraction. Given that several XLSX files could have been derived from one single patient or ECG record, it was important not to get confused about file number versus the ECG number. This is crucial at the time of machine learning analysis because several files per patient will require careful consideration to avoid data leakage issues [42]. Despite the absence of the patient-wise table in this chapter, the dataset summary provides sufficient information.

Table 3.6: Quality control criteria used for digitized ECG dataset

Quality Control Criterion	Purpose
File readability	Ensure XLSX files can be opened and processed
Numerical signal availability	Confirm extracted ECG values are present
Signal continuity	Check that waveform extraction did not produce major gaps
Recording type identification	Separate baseline and AJM/provocation files
Dataset consistency	Reduce mismatch between files and labels
Clinical relevance	Preserve important leads and morphology for Brugada Type 1

Table 3.6 This section shows the criteria for quality control that were applied to evaluate the digitalized ECG database. These criteria played an important role in increasing the quality of the database prior to the application of any preprocessing steps. This step is essential since neural networks are very sensitive to the quality of their input data.

3.12 Importance of the Digitized Dataset in This Thesis

The digitized dataset is one of the main original contributions of this thesis. Many ECG-based machine learning studies rely on existing digital ECG databases, where signals are already available in structured format [30, 31, 33]. In contrast, this work began with ECG records in PDF format and transformed them into numerical data through ECGD-based digitization. This makes the project more realistic and practically relevant because many hospitals and clinical archives store ECGs as PDF reports rather than raw digital signals.

This thesis represents the complete workflow in biomedical engineering by developing the data set in a systematic way. The process of work doesn't start from training of models; rather, it starts from data acquisition, reconstruction of analog signals into digital ones, data file creation, dataset validation, and machine learning readiness [42]. This complete process is significant because it is not just about model architectures, but also data preparation for medical AI applications.

Moreover, the digital data are crucial in diagnosing Brugada Syndrome Type 1 [4, 19]. The diagnostic criteria of Brugada Syndrome are based on the ECG

wave characteristics [4, 7], meaning that the digitalized information has to capture the QRS wave, ST wave, J-point elevation, and T wave. There is good reason for concentrating on leads V1-V3, as they are the ones mostly relevant for the diagnosis [26, 35].

The possible future extensions to this dataset include an increase in the number of ECG readings included, an improvement in digitization automation, and the inclusion of other categories like borderline cases. There is also room for the use of other advanced machine learning techniques like multi-class classification, predicting patient level results, and explainable AI. The digitization carried out in this thesis is therefore valuable not only to this project but also for future projects.

3.13 Chapter Summary

This chapter described the ECG digitization and dataset construction process used in this thesis. The original ECG recordings were provided in PDF format and required conversion into digital numerical signals before machine learning could be applied. ECGD software was used to extract waveform data from the PDF records and export the results into XLSX format. This process transformed analog ECG traces into structured time-series data.

In the chapter, the reasons for digitization were elaborated, along with the theory behind the ADC system, the function of ECGD software, signal processing, scaling, creation of the XLSX database, and quality assurance. The ultimate digitized data include 311 files in XLSX format, 167 files related to baseline ECG, 143 files related to AJM/provocation, and 1 file with an ambiguous classification.

The issues experienced during the digitalizing process include grid interference, poor image quality, scale difference, multiple page ECG report, file name ambiguity, and signal discontinuity. The issues have been solved via the method of validation and quality assurance. It is noted from the chapter that creation of dataset has been one of the significant components of the thesis and it acts as the basis of the next chapter's discussion.

Chapter 4

Preprocessing and Neural NetworkMethodology

4.1 Introduction

In this chapter, we introduce the entire method of processing and the approach of the neural network utilized in the process of automatic diagnosis of Brugada syndrome type 1 through digital electrocardiogram data. After conversion of the ECG data from PDF format to XLSX numerical format, the next critical task was the conversion of the preprocessed data to model inputs in the form of signal windows. This task had to be done since the preprocessed data in XLSX format had continuous ECG signals of varying durations and beats.

The proposed methodology for this thesis project relies on a complete machine learning approach. First, the data is read from the preprocessed dataset consisting of *Definitive* and *Non-BrS* ECG files. Next, the ECGs are loaded from XLSX files, clinically significant leads are extracted, signals are resampled at a constant frequency, ECG cleaning is performed [37, 38, 41], R-peaks and S-peaks are found, and a constant-length window is extracted from each signal centered at the S-peak [41]. Finally, a deep neural network model is trained using these processed windows.

The neural network used for this work was inspired by the MeMeA 2025 Brugada classification method [23], although the structure is adapted to be suitable for solving the binary classification problem of *Definitive / Brugada Syndrome Type 1* vs *Non-BrS*. It involves the use of convolutional layers, bi-directional LSTM layers, and an attention mechanism [27, 28, 29], which enables learning about local morphology and temporal dependency in addition to finding diagnostic regions of the signal.

This chapter covers preprocessing, splitting approach of the data set, class balancing technique, neural network model design, training parameters, optimal

threshold selection, and evaluation setup. This chapter is crucial for its relevance to the transition from the digitized ECG data set introduced in Chapter 3 to the experiments discussed in the next chapter.

4.2 Overview of the Machine Learning Pipeline

The pipeline for machine learning begins with the cleaned data set and concludes with predictions. The cleaned data set comprises two different folders that contain classes named *Definitive* and *Non-BrS*. Data inside the Definitive folder correspond to ECG signals for patients diagnosed with Type 1 Brugada Syndrome [4, 19], whereas files in the Non-BrS folder contain ECG data sets for healthy patients.

This is an effort that is geared towards ensuring that clinically significant data are retained during the conversion of the ECG data into a standard format suitable for deep learning. Given that Brugada Syndrome Type 1 diagnosis is predominantly made using right precordial leads [26, 7, 35], the pre-processing step entails working with leads V1, V2, and V3 [26]. This leads to data processing for the three leads as a multi-lead signal rather than individual channels for each of them.

The whole pipeline shows conceptually in Figure 4.1.

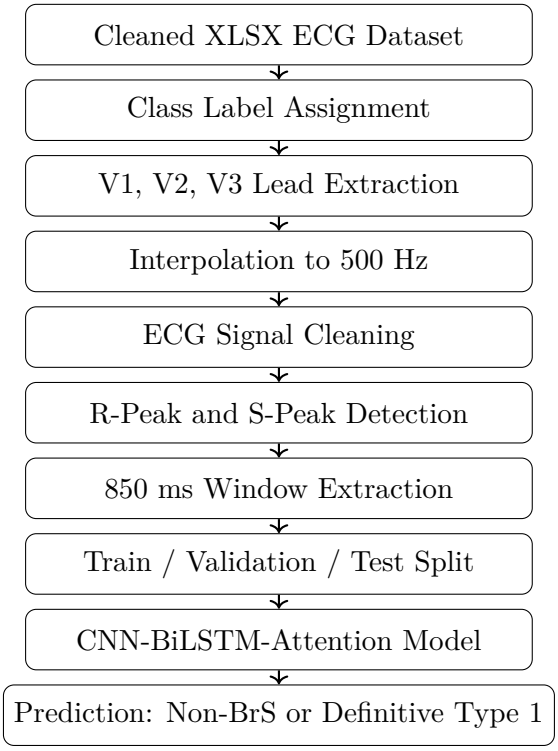

Figure 4.1: Machine learning pipeline for Brugada Syndrome Type 1 detection

This pipeline guarantees that the final input into the neural network is not the raw ECG data but rather a window within which lies the clinically significant portion of the ECG waveform [37, 38]. The reason for using the S-peak windows is that the Brugada Type 1 morphology is predominantly seen around the terminal QRS complex, J-point, ST-segment, and T wave [4, 7].

4.3 Cleaned Dataset Input

The data used in the preprocessing phase was from the cleaned data set which was obtained after the data set organization and mapping of labels phase. The raw data set had 1041 XLSX files, but the files that had valid labels were only selected. After being cleaned, 784 labeled ECG files were used. However, 257 files which lacked labels were excluded.

The clean data set was categorized into two classes. The first class was *Definitive*, which referred to ECG files that had been tagged as having Brugada Syndrome Type 1 [4, 19]. The other class was *Non-BrS*, which contained ECG files that were not classified as exhibiting the Brugada Type 1 pattern.

Table 4.1: Cleaned dataset summary

Dataset Category	**Number of XLSX Files**
Definitive / Brugada Type 1	610
Non-BrS	174
Total cleaned ECG files	**784**

Table 4.1 indicates that there is an imbalance in the distribution of the data set, whereby there were far more Definitive files compared to Non-BrS files. The problem of imbalance would need to be tackled in the training phase since a neural network trained on an unbalanced dataset tends to get biased towards the dominant class [32, 48].

4.4 Class Definition and Labeling Strategy

This classification problem for the thesis was posed as a binary supervised learning problem. Each electrocardiogram is labeled either as a *Non-BrS* or a *Definitive / Brugada Syndrome Type 1* [4, 19]. Definitive is the class used for electrocardiograms with the Type 1 Brugada signature [4, 7], while Non-BrS is the class used for electrocardiograms without it.

It should be noted that the choice of using a binary classifier in this case was made due to the primary goal of the thesis, which does not involve classifying all cases of ECGs similar to Brugada Syndrome, but only those cases that represent the Clinically Diagnostic Type 1. The Clinically Diagnostic Type 1 is the most significant case since it provides definitive confirmation of Brugada Syndrome [26, 19].

Table 4.2: Class definition used in this thesis

Label	Class Name	Description
0	Non-BrS	ECG signal without definitive Brugada Type 1 pattern
1	Definitive / Brugada Type 1	ECG signal showing diagnostic Type 1 Brugada morphology

Such a labeling scheme was also significant for interpreting the results generated by the model. As already mentioned, the result produced by the model is binary; hence, the final outcome is the probability of the window being in the Definitive category.

4.5 XLSX Signal Loading

The digital ECG files were saved in XLSX format. Each of these XLSX files had numerical ECG data which was collected from the ECG signals during the digitizing phase. The preprocessing code would read the file and check for the sheet configuration of each file. As this particular neural network model uses the leads from the right precordial site, the preprocessing step checked for the presence of V1, V2, and V3 sheets in the file [4, 26, 35].

It was expected that each lead sheet would have two main columns: the first column represented time while the second column represented the amplitude of the signal [37, 38]. In the pre-processing pipeline, the two columns were considered `x` and `y`, where `x` represents time and `y` represents voltage. This process enabled the conversion of the signals into numeric arrays.

This was also done in the loading stage by validating the files. This involved excluding files that had lead information that could not be parsed or those that lacked sufficient signal length and those with missing columns of expected leads.

4.6 Lead Selection: V1, V2, and V3

The choice of leads to examine is one of the key decision-making areas of the preprocessing phase in clinical practice. The detection of Brugada Syndrome Type 1 depends on the right precordial leads, particularly V1, V2, and V3 [4, 26, 19]. It is because these leads are located near the outflow tract of the right ventricle and are therefore crucial for Type 1 Brugada Syndrome diagnosis [7, 35].

In the proposed model, the three leads V1, V2, and V3 are considered as a multi-lead input. The model does not consider each lead independently but considers them all together in an electrocardiogram signal of three channels. This approach allows the neural network to consider not only the morphology of each of the leads but also the relationship among them since the Brugada syndrome appears in different ways in V1, V2, and V3 leads [7, 26].

In the preprocessing step, every valid XLSX file must contain all three leads. If any of these leads are absent, that file is excluded. This requirement maintains a consistent input shape for the model and avoids training on recordings with missing lead data.

Table 4.3: Lead selection strategy

Lead	**Role in This Thesis**
V1	Primary right precordial lead for Type 1 Brugada morphology
V2	Reference lead for R/S-peak detection and important diagnostic lead
V3	Additional right precordial lead supporting morphology analysis

The model in this thesis includes V1, V2 and V3 as a multi-lead input. The three leads are grouped together into one ECG segment, using 3 channels. This allows the neural network to learn the shape of each individual lead and the relationship between the leads. This is important since the Brugada pattern is not the same in V1, V2 and V3 [7, 35].

4.7 Signal Interpolation to 500 Hz

All valid XLSX files should include all three leads during the preprocessing step. If any of these leads are not present, the file is not included. This ensures a consistent input shape for the model, and prevents training on recordings where there is a missing lead.

Interpolation became important since neural networks needed inputs to have uniform dimensions [42]. The problem was that in case if there were variations in sample rates and time periods, it would become impossible to extract windows of constant length from the input signal. Interpolation allowed us to normalize all signals and have the same sampling rate for all of them [37, 38].

The proposed pipeline makes use of cubic interpolation and clamps the boundaries rather than extrapolating aggressively outside the signal range [37]. This helps in reducing boundary artifacts. Once the interpolation stage is completed, the signal is cleaned using the ECG filter.

Table 4.4: Interpolation parameters

Parameter	**Value**
Target sampling rate	500 Hz
Sampling interval	2 ms
Interpolation method	Cubic interpolation
Boundary handling	Clamped using edge values
Purpose	Standardize ECG time axis

This interpolation procedure made it possible to standardize all the ECGs before window extraction and training of the model.

4.8 ECG Signal Cleaning

After the interpolation process was complete, the ECG signal clean-up procedure took place. An ECG signal can have unwanted changes due to factors like digitization process, baseline drift, grid noise, or the actual conditions during which the ECG was recorded[37, 38].

The code for preprocessing implements ECG de-noising through the use of techniques based on NeuroKit [41]. The de-noising will be applied individually on V1, V2, and V3 after the interpolation. This ensures that the accuracy of peak detection is achieved and prevents noise from interfering with model training [41].

On the other hand, the data pre-processing method was carefully designed in such a way that no amplitude information is lost, which could have been crucial for diagnosis. Type I Brugada Syndrome has an elevation of the ST-segment, an amplitude-related characteristic [4, 7]. The window level pre-processing method subtracts the mean from the signal, eliminating the DC offset, but it does not normalize the signal by dividing it by its standard deviation.

It is a good trade-off between noise cancellation and the preservation of clinically relevant characteristics. It processes the raw ECG signals to make them suitable for

neural networks, while retaining their relevant morphology related to the QRS-ST-T complex [7].

4.9 R-Peak Detection

Detection of the R peak is essential for the analysis of the ECG because it enables identification of other waveform components [37, 38]. In this thesis, R peaks will be identified using the lead V2, which forms the reference lead in terms of extraction of windows. The selection of V2 has been made because this lead is among the best leads in relation to morphology of the QRS complex.

NeuroKit2 is used in the preprocessing pipeline to perform R-peak detection[41]. Nevertheless, the digitized ECG waveforms might have some noise and irregularities that can interfere with the automatic peak detection process. In order to address this potential issue, the code employs a fallback option, which involves the use of `scipy.signal.find_peaks` to identify any missing peaks.

This backup system is very important because of the nature of the processing of many ECG images, which can differ from one another with respect to the quality of their signals. The use of an automatic method without a backup system will lead to loss of useful data due to failure of processing some cases.

4.10 S-Peak Detection

The detection of the S-peak plays a crucial role in the method used in this study. Rather than detecting windows that start at the R-peak, the model detects windows starting at the S-peak. This approach is based on the fact that Brugada Type 1 pattern is prominently displayed after the end of the QRS complex, particularly around the J-point, ST segment, and the T wave [4, 7, 26].

Identification of the S-wave peaks was accomplished with a wavelet delineation technique using the NeuroKit2 library if applicable [41]. In case of failed detection by wavelet delineation, the algorithm resorts to finding the valley point within 100 ms after the R-wave peak, which makes physiological sense considering the close relation between the R- and S-waves.

Such a double process results in better robustness. Wavelet-based segmentation gives a more sophisticated way to do such segmentation if possible [41], whereas the alternative allows the extraction of windows even if the automatic process fails.

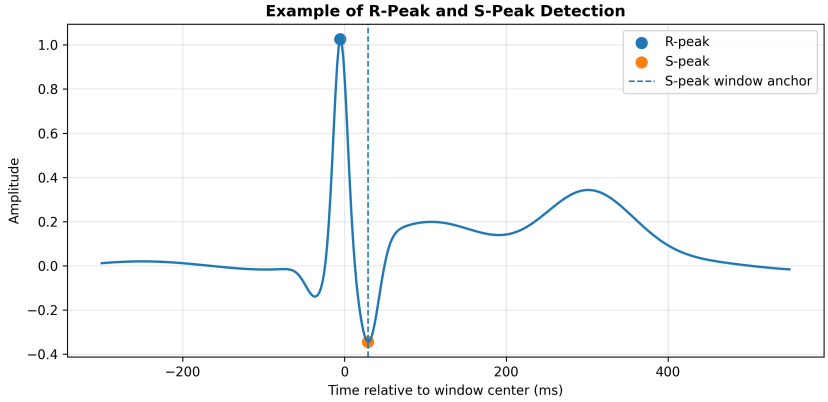

Figure 4.2: S-peak Detection Concept

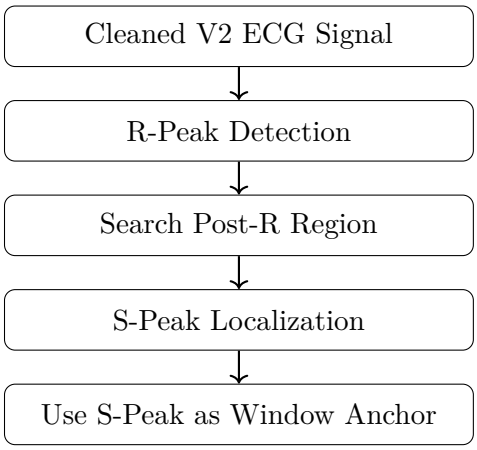

Figure 4.3: S-peak detection concept used for ECG window extraction

The S-peak focus strategy is one of the key methodological choices for this study since it concentrates on the ECG area that is essential for the appearance of Brugada Syndrome Type 1 morphology [4, 7].

4.11 850 ms Window Extraction

Once the S-peak detection stage ends, the ECG data preprocessing workflow involves taking fixed-size windows of the data around the found S-peak. The window size includes data both prior and after the S-peak. To be precise, the window consists of 300 ms prior to the S-peak and 550 ms after the S-peak, totaling 850 ms.

Assuming the sampling frequency equals 500 Hz, 850 ms of data correspond to 425 samples. However, the recorded window includes ±15 sample time shift augmentations, resulting in a recording of 455 samples per each lead. The neural network receives 425 samples from the recorded window.

It is carried out for all three leads (V1, V2, and V3) with the same anchor S-peak detected on V2. It provides temporal alignment for all three leads. Each window's size will be:

3 leads × 455 samples

During training, random time-shift cropping converts this into:

3 leads × 425 samples

For validation and testing, a deterministic center crop is used to ensure reproducibility. Figure 4.4.

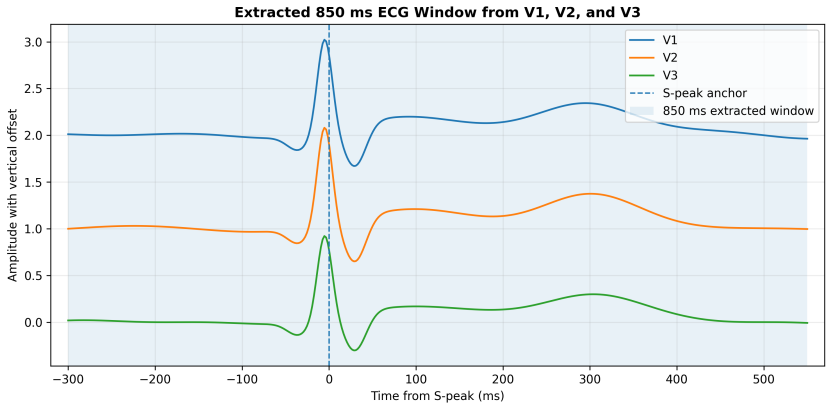

Figure 4.4: 850ms Window Extraction

Table 4.5: Window extraction parameters

Parameter	**Value**
Sampling rate	500 Hz
Pre-S segment	300 ms
Post-S segment	550 ms
Total window duration	850 ms
Stored samples per lead	455
Model input samples per lead	425
Leads used	V1, V2, V3
Reference lead for S-peak	V2

The 850 ms period is clinically significant because it contains the area where Brugada pattern type 1 morphologies occur. The part after S encompasses ST segment elevation and T wave morphology, which are important factors in classification.

4.12 Baseline Correction and Amplitude Preservation

Each extracted window undergoes baseline correction through the subtraction of the mean value from each channel [37, 38]. Through this process, the DC offset is eliminated, with the signal being centered about a particular reference level. The signal does not undergo normalization using the standard deviation. Such a step is undertaken to avoid any distortion that might be caused to amplitude changes due to such normalization.

Both the absolute and relative ST-segment elevation levels are important when diagnosing Brugada Syndrome Type 1 [4, 7, 19]. Standardizing each window according to the SD level will mean that the amount of ST segment elevation will be lost. Therefore, the preprocessing algorithm is such that relative amplitude remains unchanged and baseline level is subtracted.

This is because there is an understanding of clinical data when preprocessing is done. This is because the aim of preprocessing in this case is not to make mathematical calculations but to maintain the ECG waveform needed for diagnosis. Amplitude cannot be changed since the level of elevation plays an important role in diagnosis of Brugada syndrome [4, 7, 26].

4.13 Time-Shift Augmentation

Temporal augmentation was applied in order to improve robustness [42]. Since it may not always be possible to perform S-peak detection perfectly, there needs to be some tolerance towards minor temporal shifts in the positioning of the window. In order to achieve this, a ± 15 sample padding is added at both ends of each saved window. This results in an input size of 425 samples after training.

At a rate of 500 Hertz, 15 sets would be equivalent to around 30 milliseconds. The addition simulates small movements in S-peak location but retains the morphology of the ECG signal. However, what is most important is that the exact same time shift is used for leads V1, V2, and V3.

There is no increase in amplitude. It is clinically relevant because any artificial manipulation of amplitude would cause the ST-segment elevation to be distorted [4, 7, 19], hence the importance of Brugada type 1 diagnosis. Therefore, time-shift amplification strengthens the time-domain aspect without affecting amplitude analysis.

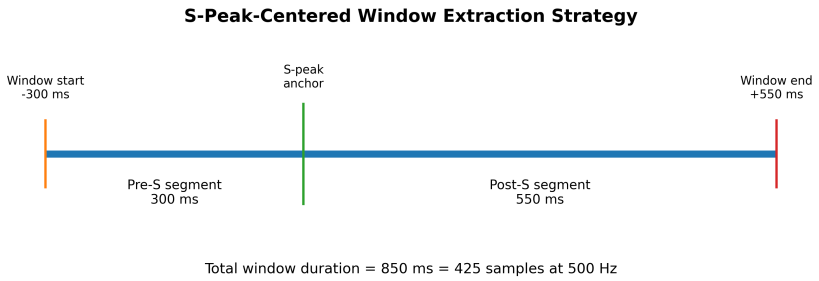

Figure 4.5: Time Shift Augmentation

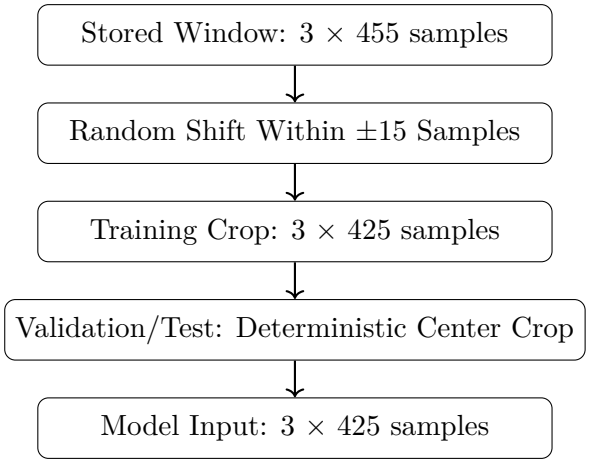

Figure 4.6: Time-shift augmentation and deterministic center cropping

This particular technique not only improves the ability of the algorithm to generalize but ensures the maintenance of the biological fidelity of the ECG signal.

4.14 Train, Validation, and Test Split

The dataset was split up into training, validation, and test datasets [42]. Splitting up was done on a recording basis rather than a window extraction basis. It is essential to note this point since more than one window or page could have been generated from the same ECG recording. If such data is used in the training set and test set, there could be an increase in the accuracy due to data leakage [42].

This problem is overcome by grouping files based on their base names before performing any splits. This way, all the pages for a particular recording get into one split. This process ensures that unseen recordings will form part of the test set and not seen ECG windows during training.

The processed data was saved as NumPy arrays in the `processed_data` folder. This comprised the `X_train`, `X_val`, `X_test`,along with their corresponding labels arrays.

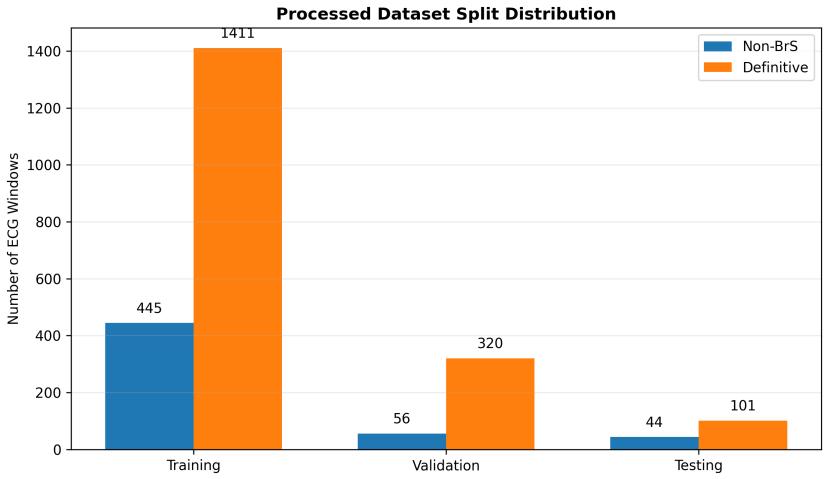

Figure 4.7: Train, Validation and Test Split

Table 4.6: Processed window dataset split

Split	Total Windows	Non-BrS	Definitive
Training	1856	445	1411
Validation	376	56	320
Testing	145	44	101
Total	**2377**	**545**	**1832**

Table 4.6 From the analysis, it is clear that 784 processed ECGs generated 2,377 heartbeats-based windows of ECGs after preprocessing. This data set is skewed since there are more instances of Definitive class compared to the Non-BrS class [32, 48].

4.15 Class Imbalance Handling

Class Imbalance is a problem that is often faced when implementing machine learning for medical purposes [32, 48]. In our current data set, there is an imbalance of more Definitive cases compared to Non-BrS cases. The problem with not taking

care of the class imbalance is that the model might have a bias toward predicting the majority class [32, 48].

This problem is addressed through the use of `WeightedRandomSampler` in the PyTorch DataLoader. This is because the class with the fewest examples will be given higher weights in terms of sampling to balance the batches during the training process. Oversampling is not done for the validation and testing set because they have to be realistic [42].

The computation of the class weights and the use of the sampling technique happen only based on `y_train` without any interference from the validation/test sets and this avoids any data leakage during training [42].

It helps the model learn from the Non-BrS class samples better during the training process without compromising the original distribution when evaluating the model.

4.16 Neural Network Architecture Overview

The neural network model used in this thesis uses a combination of architectures including Conv1D, Bidirectional LSTM, and Attention [27, 28, 29, 23]. The input to the model is an ECG multi-lead window with the dimensions of:

$$3 \text{ leads} \times 425 \text{ samples}$$

The three signal paths include leads V1, V2, and V3 [4, 26, 35]. The dataset consists of 425 points which are from 850 milliseconds cropped from 500 Hz sampling rate.

The model architecture starts off with the convolutional layers where local features of the ECG waveform will be extracted [27]. Then comes the bidirectional long short-term memory (LSTM) layer in order to capture any dependencies along the ECG sequence [28]. Later on, an attention layer will be used to determine the weightage of each point in time [29].

The structure of this network is suited for ECG classification because it includes features such as morphological extraction locally, sequence modeling temporally, and interpretable attention [27, 28, 29, 23].

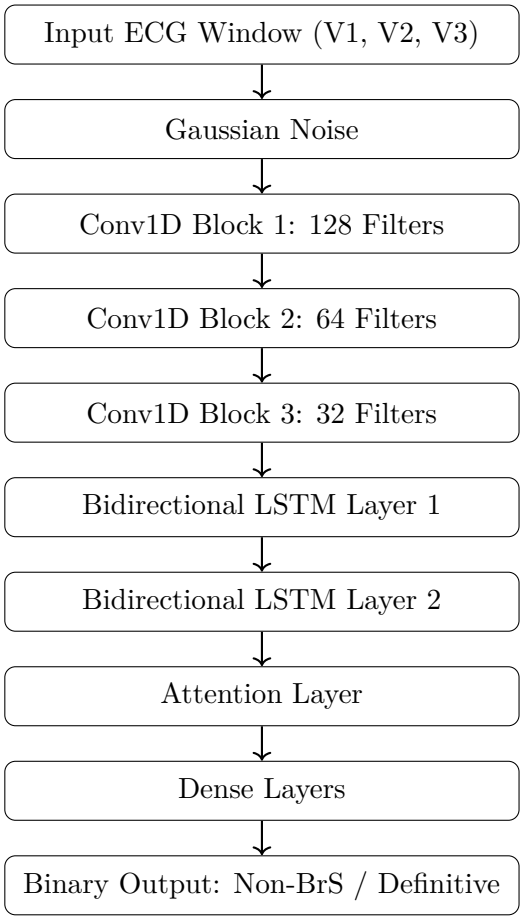

Figure 4.8: CNN-BiLSTM-Attention neural network architecture

4.17 Convolutional Feature Extraction

The first section of this neural network model consists of three convolutional blocks. The number of filters used in the first, second, and third convolutional blocks are 128, 64, and 32, respectively. Every block consists of convolutional layer, batch normalization, ReLU activation, max pooling, and dropout layers [27]. The neural network is confirmed to contain three convolutional layers with three channels: V1, V2, and V3.

One of the major advantages of using convolutional layers is the ability of such filters to detect local features within electrocardiograms [27]. Local features may include characteristics such as the steepness and length of the QRS complex, the slope of the ST segment, and the shape of the T wave. Such local features are automatically detected by convolutional filters.

Max pooling helps reduce the temporal component and also helps in maintaining

prominent features, thus reducing the computational burden [27]. The dropout technique is used to prevent overfitting by randomly turning off parts of the neural network.

Table 4.7: Convolutional feature extractor

Block	**Filters**	**Kernel Size**	**Additional Operations**
Conv Block 1	128	3	BatchNorm, ReLU, MaxPool, Dropout
Conv Block 2	64	3	BatchNorm, ReLU, MaxPool, Dropout
Conv Block 3	32	3	BatchNorm, ReLU, MaxPool, Dropout

The convolutional feature extractor translates the ECG window in its original form to a representation which can be temporally modeled [27].

4.18 Bidirectional LSTM Layers

After the convolutional blocks, two BiLSTM layers are added to the network architecture. The output from the convolutional feature extractor is then transposed in such a way that the time dimension is arranged properly for processing using the LSTM layers. Two BiLSTM layers are used, each having 32 neurons. Since the LSTMs are bidirectional in nature, the resultant representation captures information in both temporal directions [28].

It is crucial to apply BiLSTM layers due to the time-dependent nature of ECG analysis [28, 37, 38]. For example, the ST segment has to be analyzed in connection with the QRS complex that preceded it and the T wave that followed [7]. The use of a bidirectional model enables the acquisition of dependencies from both past and future windows [28].

This feature is especially useful in detecting the type 1 pattern of Brugada because the diagnosis of this pattern does not depend on any one particular point but spans the entire period between the QRS-ST-T waveforms [4, 7, 26]. Through these BiLSTM layers, the model learns about these connections.

4.19 Attention Mechanism

This is achieved by designing a custom attention layer, added after the BiLSTM layers. The attention process gives weightage to different time steps in the sequence.

This helps in understanding how much significance should be attached to different sections of the ECG window [29].

The attention mechanism that has been developed creates an intermediate feature representation [29] using a learned weight matrix and bias, computes attention values, normalizes these values using the softmax function to derive attention weights, and finally creates a context vector using a weighted average of the BiLSTM outputs.

With respect to the detection of Brugada Syndrome Type 1, the attention component has clinical importance since the model will pay attention to the QRS-ST-T section [4, 7, 26]. Attention maps can then be generated and analyzed to determine if the model is paying attention to realistic areas of the ECG [29, 23].

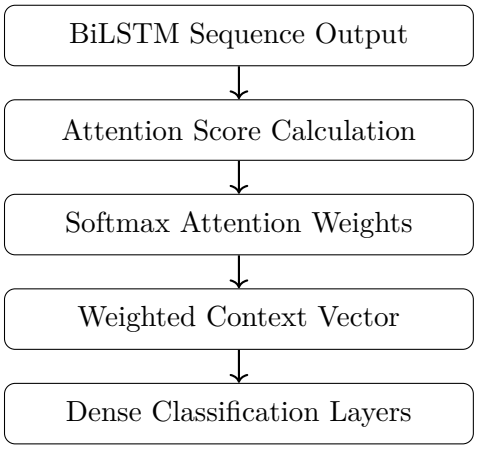

Figure 4.9: Attention mechanism used for temporal ECG interpretation

This is because of the attention mechanism, which helps in increasing model interpretability since the process of making predictions makes use of visualization of the temporal focus of the model being evaluated [29, 23].

4.20 Dense Classification Layers and Output

Once the model produces a context vector after going through an attention layer, it is then fed through three dense layers. All three dense layers contain 32 neurons, and after each layer comes batch normalization, rectified linear unit, and dropout.This is where the learned temporal and morphological characteristics get integrated into a small feature set suitable for classification [27, 28, 29].

The final output layer consists of one neuron which produces the logit output. While testing the model, the logit output undergoes transformation by the use of the sigmoid function to obtain a probability between zero and one [42]. Further,

the result undergoes classification into either Non-BrS or Definitive based on a set threshold value [32]. The model code confirms the binary linear output layer with one output.

Table 4.8: Model architecture summary

Component	**Configuration**
Input	3 leads × 425 samples
Gaussian noise	1% noise during training
Conv Block 1	128 filters
Conv Block 2	64 filters
Conv Block 3	32 filters
Recurrent layers	2 Bidirectional LSTM layers
Attention	Custom additive attention
Dense layers	3 dense layers with BatchNorm and Dropout
Output	Single binary logit

The structure allows the integration of low-level ECG morphology along with temporal information and attention-based explainability [27, 28, 29, 23].

4.21 Training Configuration

The network was trained using PyTorch. In the training script, deterministic settings were used to improve reproducibility, where the random seeds for Python, NumPy, and PyTorch were set. If GPU availability was detected, then the CUDA determinism was also set.

The training was done using AdamW optimizer with learning rate = 0.001 and weight decay = 0.02 [50]. The weight decay acts as a form of regularization to avoid overfitting [42]. During the final training, BCEWithLogitsLoss was used which is ideal for tasks dealing with binary classification and uses logits. Even though focal loss was introduced in experimental purposes, the training was conducted using binary cross-entropy with logits [42].

The network was trained up to 50 iterations, using early stopping based on validation metrics [42]. The best-performing network was selected on the basis of AUPRC for the validation set. Such an approach is justified considering the class imbalance problem in the data, because AUPRC is a better metric than accuracy in such cases [32, 48].

Table 4.9: Training configuration

Parameter	**Value**
Framework	PyTorch
Optimizer	AdamW
Learning rate	0.001
Weight decay	0.02
Loss function	BCEWithLogitsLoss
Batch size	64
Maximum epochs	50
Early stopping patience	10
Model selection metric	Validation AUPRC
Class imbalance handling	WeightedRandomSampler

The above training setup is based on ensuring that there was equilibrium between stability, generalization, and the minority class sensitivity.

4.22 Threshold Optimization

Generally, the threshold used in a binary classifier is 0.5 [42]. However, in the context of medical classifiers, it may not necessarily be 0.5 since there is imbalance between the cost of having false negative results compared to having false positive results [32, 48]. For instance, failing to detect a case of Brugada Type 1 can be more serious than misdiagnosing a patient.

With this view in mind, the pipeline of training includes threshold optimization using receiver operating characteristic (ROC) curve and Youden's J statistic [51, 32]. Youden's J is defined as:

$$J = \text{True Positive Rate} - \text{False Positive Rate} \tag{4.1}$$

[51]

The best operating point is where the maximum value for the metric mentioned above can be attained [51]. The process entails computing ROC values using the validation dataset, identifying the threshold, saving the ROC curve, and storing the threshold in `threshold.npy`.

Such an optimized threshold will be used during evaluation. Using a validation approach to determine the threshold results in a better outcome for classification as compared to the objective and data set [32, 48].

4.23 Evaluation Preparation

Even though the final outputs are shown in Chapter 5, the evaluation system remains a part of the methodology. In evaluating the model, it is important to load the trained model using the saved checkpoint and the optimal threshold obtained from the `threshold.npy` file. If no threshold is available, the evaluation script falls back to the default threshold of 0.5 [42].

Prediction scores are created using sigmoid probability values and the best threshold [42]. Afterward, the classification report and confusion matrix are produced [32]. Attention weights are also collected and used to create attention maps over the ECG segments [29, 23]. Attention entropy is computed in order to measure the level of attention focus and uniformity.

This preparatory evaluation is helpful for conducting both quantitative and interpretation-based analyses [32]. Quantitative analysis will help us understand the performance of the model, whereas visualization based on attention will enable an inspection of ECG segments that contributed to making these predictions [29, 23].

4.24 Methodological Strengths

However, there are some strengths in the methodology described in this thesis. Firstly, this methodology is based on clinical knowledge and specifically focuses on V1, V2, and V3 leads since they are most relevant in the case of Brugada Type 1 [4, 26, 35]. Secondly, the method considers a window around the S peak and not some random ECG part, so it ensures that the QRS-ST-T segment is included [4, 7].

Third, the multi-lead input is utilized to help learn relationships between the signals at leads V1, V2, and V3. Fourth, the issue of class imbalance is dealt with using weighted sampling while training the neural network model [32, 48]. Fifth, the use of attention mechanisms is considered as a means towards achieving interpretability [29, 23]. Finally, the method of splitting data avoids data leakage.

Together, all of these methodologies make up a comprehensive pipeline for automated detection of Brugada Syndrome Type 1.

4.25 Chapter Summary

In this chapter, the methodologies related to the preprocessing of the dataset and the neural networks used in this research will be discussed. The preprocessed dataset was retrieved in XLSX files, which can be divided into Definitive and Non-BrS folders. The V1, V2, and V3 leads have been selected, considering their significance regarding the detection of Brugada Syndrome Type 1.Interpolation of

the signals was performed up to 500 Hz frequency and they were filtered for noise reduction, followed by analysis using R-Peak and S-Peak detection.

850 ms fixed windows were obtained for each identified S-peak signal. Each saved data window had three channels of 455 data points for each channel with the augmentation buffer of time shift applied. The training process involved random time shift cropping, which produced model inputs with 425 sample points, while the test set used centered crop method.

The preprocessed data set contained 2377 ECG window samples, which were subsequently divided into training, validation, and test sets. The deep learning model included Conv1D, bidirectional LSTM, custom attention layer, dense, and binary classifier layers. For training the model, we used AdamW optimizer, BCE-WithLogitsLoss, weighted sampling, early stopping, and AUPRC score on validation set to select the best model.

This chapter contains the findings from the experiment on the proposed model and involves a discussion on the classification accuracy, confusion matrix, ROC curve, sampling distribution, and the attention map.

Chapter 5

Results and Evaluation

5.1 Introduction

This chapter outlines the findings from the experiments carried out on the proposed deep learning model that seeks to detect Brugada Syndrome Type 1 through digitized electrocardiogram (ECG). After digitizing, cleaning, preprocessing, extracting windows with the center at the S-peak, and training the neural network, the last stage of the experiment was testing. The main goal of this chapter is to evaluate the performance of the proposed CNN-BiLSTM-Attention model in classifying Definitive or Brugada Type 1 ECG windows from Non-BrS ECG windows.

The evaluation was based on the final processed test dataset generated as part of the preprocessing phase. The data used in the evaluation included an ECG window from the leads V1, V2, and V3. These windows were focused on the S-peak and arranged such that the QRS-ST-T zone remained intact, which is considered important for the Brugada Type 1 morphology. Hence, the design of the model and the process of preprocessing was evaluated in terms of both computing and clinical aspects.

The evaluation method used a number of performance indicators in terms of accuracy, precision, recall, F1 score, area under curve of ROC, and confusion matrix analysis [32, 48]. Such performance indicators were selected because accuracy alone is inadequate in evaluating medical classifiers, especially when there is class imbalance. In this experiment, the number of instances of Definitive/ Brugada Type 1 was higher than Non-BrS instances. Hence, class-wise evaluation becomes necessary. Recall became an important parameter in view of the serious consequences of a missed Brugada Type 1 diagnosis.

Apart from numerical assessment, in this chapter, there is a use of visuals such as the confusion matrix, the receiver operating characteristic (ROC) curve, sampling empirical cumulative distribution function (ECDF), and attention maps. The

confusion matrix indicates how the model made its prediction, whether accurate or not. The ROC curve depicts the discrimination power of the model and is useful in determining the optimal threshold. The ECDF shows the role of the weighting approach used in sampling towards making the training process balanced.

In this chapter, an evaluation of the proposed approach is conducted, both in terms of its prediction accuracy and interpretability. From the results, it can be observed that the proposed model performs well in predicting the Definitive / Brugada Type 1 class but also highlights other issues related to it.

5.2 Evaluation Setup

This evaluation scheme was put in place in order to perform an evaluation of the trained neural network on ECG windows that have never been seen before. The model used for the evaluation task was the highest performing model from the CNN-BiLSTM-Attention models obtained through training. In the evaluation process, this model was reloaded from its respective checkpoint and used to evaluate the test data set. The other parameter that was used was the decision threshold which had been optimized in training.

Input to the model included the ECG windows from channels V1, V2, and V3. Each data sample included a dimensionality of 3 channels $\times$ 425 data samples. The input was determined due to preprocessing of the ECGs where interpolation was done at 500 Hz, followed by denoising and segmentation at the S-peak point.

The evaluation was performed using only the test set. It is very important since the test data were not used at all for the purpose of training or validation of the model. The approach for splitting the data was chosen in such a way as to ensure that no data leakage happened. For this, files were classified based on the base name of the recording before splitting into parts. In consequence, no two or more pages/windows from one recording could end up in different sets.

For this purpose, the appropriate threshold value was determined based on the validation ROC curve along with Youden's J statistic [32, 48]. After determining the threshold, it was used for testing purposes. It is essential to optimize the threshold in cases of medical classification since using 0.5 threshold might not lead to obtaining the best tradeoff in terms of sensitivity and specificity [51, 32]. In the classification of Brugada Syndrome Type 1, missing true Definitive patient has significant consequences.

Table 5.1: Evaluation setup summary

Evaluation Component	Description
Model used	Best saved CNN-BiLSTM-Attention model
Input leads	V1, V2, V3
Input size	3 leads × 425 samples
Test data	Unseen ECG windows
Output classes	Non-BrS and Definitive / Brugada Type 1
Threshold method	Validation ROC curve using Youden's J statistic
Evaluation metrics	Accuracy, precision, recall, F1-score, ROC-AUC
Visual outputs	Confusion matrix, ROC curve, sampling ECDF, attention maps

The proposed evaluation framework made it possible for the model to be tested using two perspectives: machine learning and clinical interpretation. The former was done through numerical measures, whereas the latter was aided by visualization techniques.

5.3 Test Dataset Composition

Final Test Dataset The final test dataset consisted of 145 ECG windows that were selected from the clean ECG data set after data processing. The test data set was comprised of two classes; one was called Non-BrS and the other was Definitive / Brugada type 1. Class Non-BrS had 44 ECG windows, while class Definitive had 101 ECG windows.

Class imbalances were noted in the test set because there were more Definitive cases compared to Non-BrS cases. The imbalances noted were based on the general makeup of the classes for the cleaned dataset as well as the ECG windows that were extracted from the data. Class-wise Precision, Recall, and F1 score were thus more helpful than Accuracy because, if Accuracy alone was looked at, it would be hard to assess the model's performance in the minor class [32, 48].

Table 5.2: Test dataset composition

Class	Number of Test Windows
Non-BrS	44
Definitive / Brugada Type 1	101
Total	**145**

The distribution of test data suggests that there were an appropriate number of samples taken from each class, though it was noted that the Definitive class had higher frequency than the other. This explains why it is crucial to consider the macro and weighted averages during the evaluation process.

5.4 Classification Report

The output of classification report contains all the numeric values related to the evaluation of the model. This includes the metrics such as precision, recall, f1-score, and support values corresponding to each label. Precision refers to the correctness of the predicted samples belonging to a certain class, while recall refers to the correctness of the true samples belonging to a certain class. The F1-score is combines precision and the recall into a single balanced measures [32].

Accuracy of the final model for the test data is 82%. Regarding the Definitive / Brugada Type 1 class, accuracy is 0.89, recall is 0.85, and F1 score is 0.87. This suggests that the performance of the classifier in this case is very good since Brugada Type 1 ECG windows have been detected quite effectively. In turn, the classifier's precision in terms of the Non-BrS class is 0.69, recall is 0.75, and F1 score is 0.72. It should be noted that the performance in terms of Non-BrS was lower than the one for Definitive since Non-BrS was a minority class.

Table 5.3: Classification report on test dataset

Class	Precision	Recall	F1-score	Support
Non-BrS	0.69	0.75	0.72	44
Definitive / Brugada Type 1	0.89	0.85	0.87	101
Accuracy	–	–	**0.82**	**145**
Macro Average	**0.79**	**0.80**	**0.79**	**145**
Weighted Average	**0.83**	**0.82**	**0.82**	**145**

These results indicate that the model is better able to detect the Definitive

class compared to the Non-BrS class. It is clinically significant since one of the objectives of this study is to find Brugada Syndrome Type 1. The F1 score for Definitive class being 0.87 means that the model is able to recognize the Type 1 Brugada ECG patterns.

The macro F1 score was 0.79, whereas the weighted F1 score was 0.82. This variation between the two scores can be attributed to the imbalance that exists within the testing dataset. As the Definitive class had many more instances than the other one, the influence of the Definitive class results is more prominent when calculating the weighted F1 score.

In summary, the results of the classification report clearly suggest that the developed model has the capability of detecting the presence of Brugada Type 1 syndrome from digitized ECG signal windows, although with room for improvement in the area of Non-BrS performance due to insufficient Non-BrS samples.

5.5 Confusion Matrix Analysis

The confusion matrix gives a clear picture of both correct and wrong predictions of classes [32]. It indicates how many samples belonging to each class have been classified as either Non-BrS or Definitive classes. This tool is quite helpful in medical diagnostics since it enables us to examine both false positive and false negative cases separately.

The confusion matrix of the final test prediction is presented in Figure 5.1.

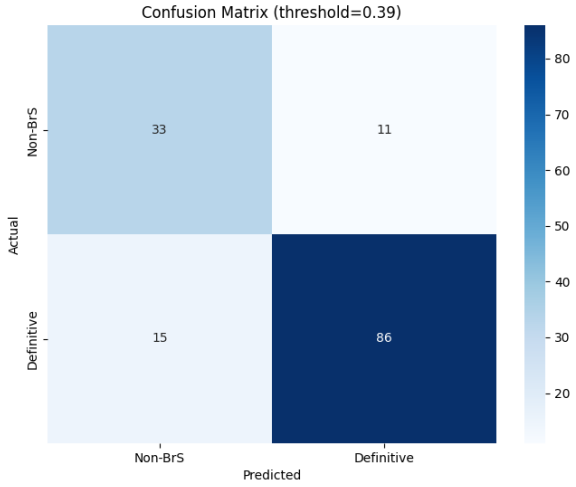

Figure 5.1: Confusion matrix of the proposed CNN-BiLSTM-Attention model on the test dataset

The confusion matrix values are summarized in Table 5.4.

Table 5.4: Confusion matrix values

Actual / Predicted	Non-BrS	Definitive
Non-BrS	33	11
Definitive	15	86

In the case of Non-BrS, there were 33 true positives from this category that were predicted to be in the Non-BrS category, and there were 11 false positives where patients were predicted to have Definitive BrS even though they did not belong to this category. In other words, the false positives are cases where the prediction of having Brugada Type 1 is incorrect since their true category is Non-BrS.

From the Definitive category, there were 86 positive diagnoses, whereas there were 15 negative diagnoses that are false negatives from the Definitive category. For Brugada Syndrome Type 1 diagnosis, the false negatives are very significant due to the fact that they denote the false identification of the patient not having Brugada Type 1 morphology which may pose a threat to the patients.

The confusion matrix validates the findings from the classification report. In terms of correct predictions, the algorithm performed well on Definitive samples and on the primary class. There were some Definitive samples that failed to be identified by the model, along with some samples from the Non-BrS class misclassified as Definitive.

5.6 ROC Curve and Threshold Optimization

For the purpose of determining how well the classifier distinguished the two classes at various threshold levels, the Receiver Operating Characteristic curve, better known as the ROC curve, was employed [32]. As opposed to using a single threshold level, the ROC curve displays how the true positive rate varies against the false positive rate at various threshold levels. The reason for doing this is that the optimal threshold level for a medical classification task need not necessarily be 0.5.

Threshold optimization was accomplished by means of Youden's J statistic in this thesis. Youden's J equals the true positive rate minus the false positive rate. The threshold value that achieves the maximum Youden's J balances the sensitivity and specificity tradeoff. [51]

The ROC curve is presented in Figure 5.2.

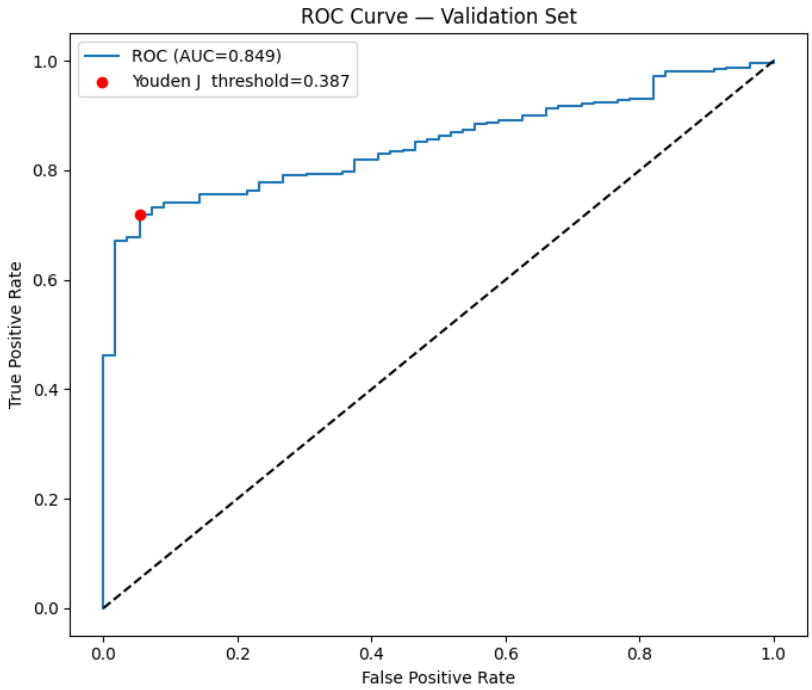

Figure 5.2: ROC curve and optimized threshold selection using Youden's J statistic

Table 5.5: ROC and threshold summary

Parameter	**Value**
ROC-AUC	0.849
Optimized threshold	0.387 / approximately 0.39
Threshold method	Youden's J statistic
Evaluation use	Threshold selected on validation ROC and applied during test evaluation

From the value of ROC-AUC = 0.849, it can be observed that there is excellent discrimination between the Non-BrS and Definitive ECG window classes. The higher the value close to 1, the better the separability between two classes; the closer the value is to 0.5, the lower the discrimination power of the classifier.

The optimal threshold value is about 0.39. What it implies is that the sample will be classified under Definitive category if the predicted probability was above the threshold value. The threshold value is below 0.5 which shows that there was

improvement in the sensitivity level at which the Definitive class was detected. It could be helpful in the context of medical classification because the misclassification cost might be higher compared to detection cost.

5.7 Sampling ECDF Analysis

The use of sampling ECDF graph was done in order to study the influence of weighted sampling during the training process. Given that there were more samples of one class compared to others in the dataset, weighted sampling during training was conducted using WeightedRandomSampler [32, 48]. The aim was to change the class ratio in training but not during validation and testing.

The sampling ECDF plot is presented in Figure 5.3.

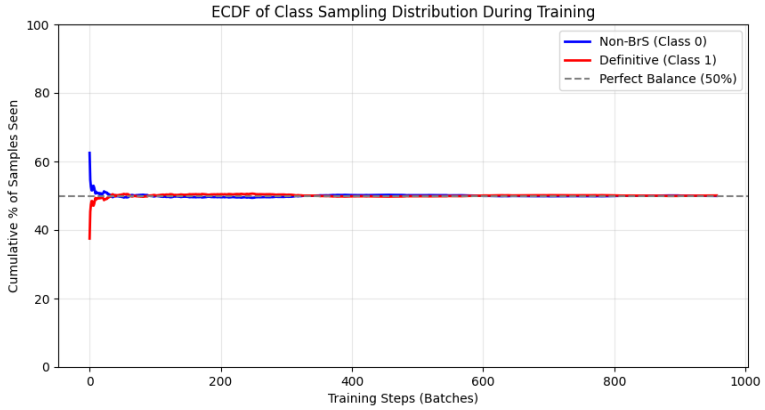

Figure 5.3: Class sampling ECDF showing the effect of weighted sampling during training

This can be observed in the graph above which displays the evolution of the cumulative percentage of samples in each category during the training process. It is expected that due to the use of weighted sampling, the model will not encounter samples of majority class only. It is evident from the graph that the distribution of categories is much more balanced during the training process.

It was particularly critical that there was an objective for which weighted sampling could be used since the number of instances for the Non-BrS category was less than that in the Definitive category. In the absence of any sampling technique, the model may be trained to favor predictions for the majority class, thereby giving low accuracy for the Non-BrS category.

It must be stressed that the approach of oversampling was used on the training set but not on the validation or testing sets. This is essential since the purpose of

evaluation is to assess how well the algorithm performs on an unbiased dataset.

5.8 Attention Map Visualization

Attention maps have been used to make the model more interpretable [29], specifically the CNN-BiLSTM-Attention model. Attention allows the assigning of weight to each of the time windows within the ECG window. This allows visualization of the parts of the ECG window that affect the model's output.

Regarding attention visualization for diagnosing Brugada Syndrome Type 1, it is relevant for the clinic because, according to the model, it will be necessary to pay particular attention to the area of interest between the QRS-ST-T segments. The window of attention has been selected based on the S-peak, which includes the terminal QRS, J point, ST segment, and T wave.

5.8.1 Attention Maps for Non-BrS Samples

Figure 5.4 and Figure 5.5 show attention maps for correctly classified Non-BrS samples.

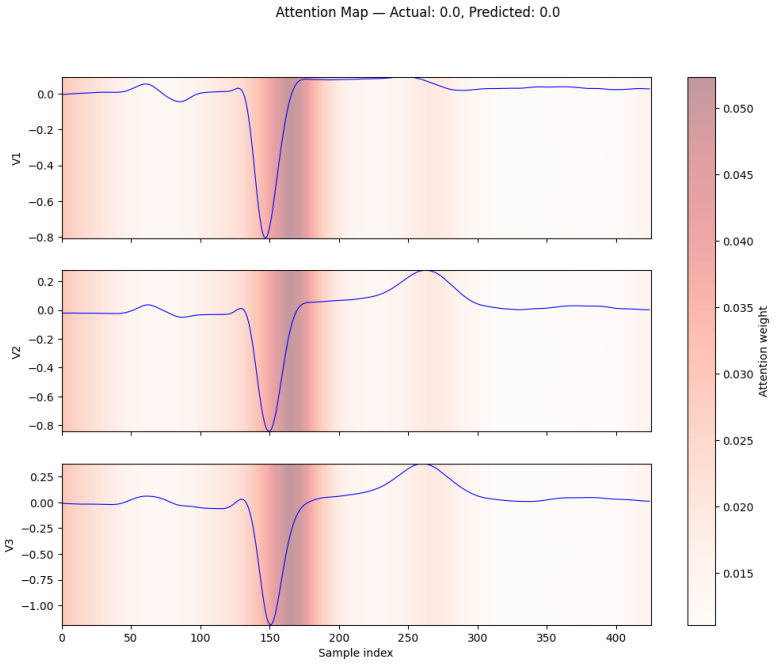

Figure 5.4: Attention map visualization for a correctly classified Non-BrS ECG sample

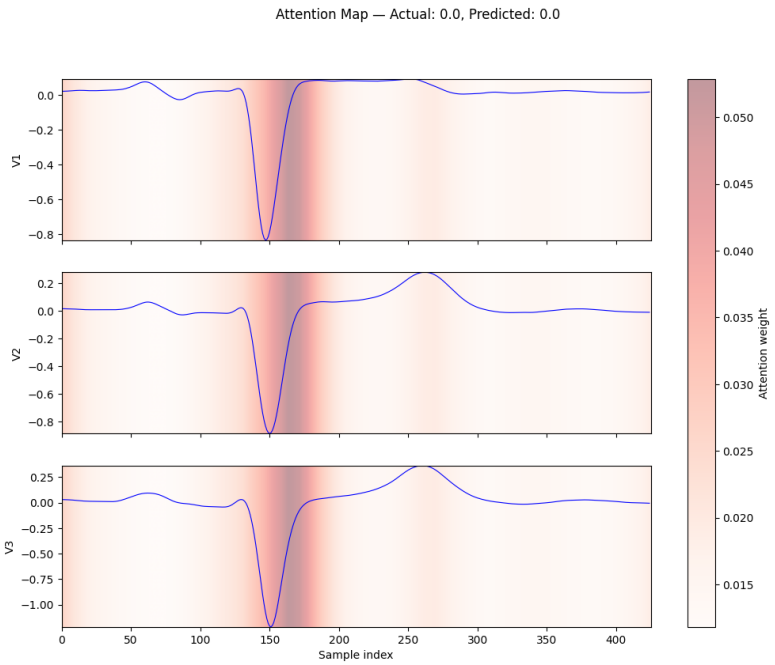

Figure 5.5: Attention map visualization for another correctly classified Non-BrS ECG sample

In these cases of Non-BrS, the attention map visualizations reveal how the model spreads its attention over the ECG signal. As we know that these signals lack the clear-cut Brugada Type 1 waveform, it follows that the model's classification would be contingent upon the lack of coved ST segment. In this case, attention visualization offers an opportunity to observe if the model is basing its judgment on signal morphology alone.

5.8.2 Attention Maps for Definitive Brugada Type 1 Samples

Figure 5.6 and Figure 5.7 show attention maps for correctly classified Definitive / Brugada Type 1 samples.

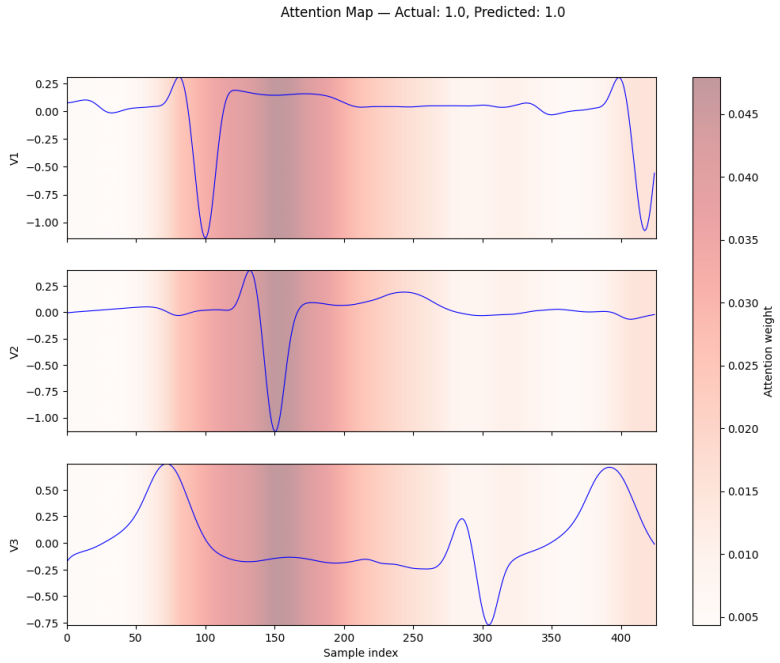

Figure 5.6: Attention map visualization for a correctly classified Definitive Brugada Type 1 ECG sample

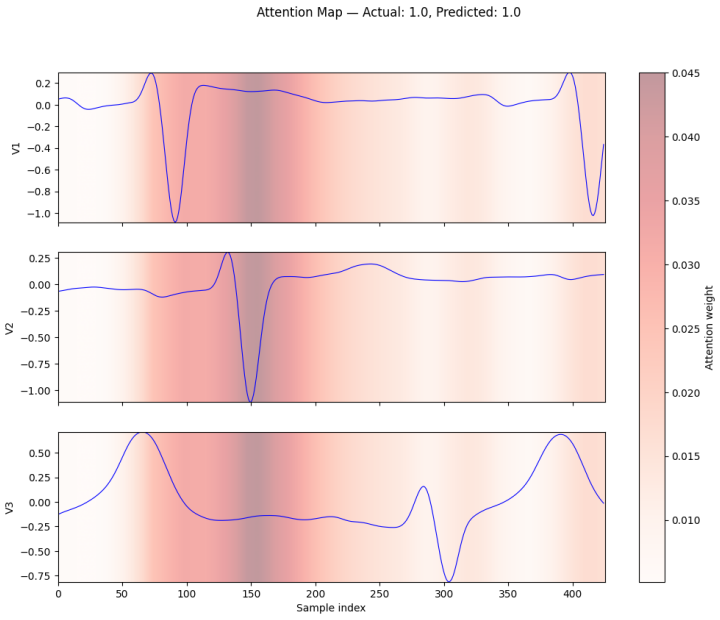

Figure 5.7: Attention map visualization for another correctly classified Definitive Brugada Type 1 ECG sample

In the case of Definitive samples, attention weights will be focused on areas adjacent to the post QRS complex part of the signal, specifically the ST segment and T-wave area. This is because the Type 1 Brugada morphology occurs at these regions. Hence, attention maps will be helpful in evaluating the clinical plausibility of the model's prediction.

Interpretation of attention maps requires caution. Attention maps do not imply causation [52], and an attention score is not a guarantee of similarity between the model's approach and that of a cardiologist. Instead, attention maps must be treated as visual evidence to help with model analysis.

Additional attention maps, such as `sample_47_cls1.0.png`, `sample_48_cls1.0.png`, and `sample_50_cls1.0.png`, can be included in the appendix.

5.9 Error Analysis

Though the model performed very well, some errors can still be observed in the confusion matrix provided below. The common types of errors found in this model include False Positives and False Negatives. A false positive is one wherein the actual class label is Non-BrS but the predicted class label is Definitive.

Table 5.6: Error type summary

Error Type	**Count**	**Meaning**	**Possible Impact**
False Positive	11	Non-BrS predicted as Definitive	May lead to unnecessary clinical review
False Negative	15	Definitive predicted as Non-BrS	May miss a Brugada Type 1 pattern
Total errors	**26**	Incorrect predictions out of 145 test samples	Indicates remaining model limitations

The positive results indicate that some of the ECG windows that were not related to the Brugada syndrome had shapes which were misinterpreted by the program as being consistent with Brugada Type 1. It might happen due to such changes in the ECG of the healthy patient as noise, alteration in the ST-segment or conduction disturbances. False positives are generally not welcome in the clinical setting, but can be acceptable in the screening environment.

The false negative examples are more clinically relevant since they indicate definite morphologies that were not recognized by the model. This might happen because the type 1 Brugada morphology could be weak, noisy, partly hidden, or

not well-represented in the window where it was sampled. Additionally, the false negatives could occur as a result of variations in digitization quality or class overlap.

Both errors are present at the same time, hence suggesting that the suggested approach cannot be used as an alternative to clinical diagnosis but only serves as an auxiliary means for making decisions in the course of the analysis of ECG signals.

5.10 Results Summary

The performance achieved by the proposed CNN-BiLSTM-Attention model is impressive when it comes to detecting automatically Brugada syndrome type 1 in patients. For the testing data set, the performance of the algorithm was quite high with accuracy of 82%. However, it was especially impressive when used on the Definitive class with Precision 0.89, Recall 0.85, and F1-score of 0.87.

Table 5.7: Final result summary

Metric	**Value**
Accuracy	82%
Definitive precision	0.89
Definitive recall	0.85
Definitive F1-score	0.87
Non-BrS precision	0.69
Non-BrS recall	0.75
Non-BrS F1-score	0.72
ROC-AUC	0.849
Optimized threshold	Approximately 0.39
Test samples	145

These results clearly indicate that the developed model can learn patterns associated with the Brugada Type 1 pattern successfully. It is important to note that the very high F1-score achieved by the Definitive class is crucial because recognizing the Type 1 pattern Brugada pattern is the main goal of the thesis. However, the model performed less effectively in relation to the Non-BrS class. This fact shows that more Non-BrS data may be needed in further research.

The ROC-AUC of 0.849 is another testament to the efficacy of this model at differentiating between these two categories. The optimization of the threshold around 0.39 made for better classification as compared to the mere default threshold. The confusion matrix showed that there was a good number of Definitive instances being correctly classified, but some false negatives were also present.

The attention maps provided qualitative interpretability, showing the areas in the ECG windows where the model was paying attention. Though attention maps cannot be directly used as clinical reasoning, they provide us with very useful information regarding the functioning of the model.

On the whole, the outcome of this experiment proves that the use of digital electrocardiograms (ECGs) in combination with the deep learning approach can provide accurate automated recognition of Brugada Syndrome Type 1. In addition, this experiment highlights the importance of exact digitization, preprocessing, selection of windows around S-peak, addressing imbalance issue, decision threshold tuning, and interpretability analysis.

5.11 Chapter Summary

The findings from the evaluation of the CNN-BiLSTM-Attention framework for Brugada Syndrome type 1 detection have been presented in this chapter. The analysis was conducted using a test dataset of 145 windows consisting of 44 Non-BrS and 101 Definitive cases. The model achieved an accuracy rate of 82%.

According to the classification report, the accuracy for the Definitive / Brugada Type 1 category is high as its precision, recall, and F1 score are 0.89, 0.85, and 0.87 respectively. The precision, recall, and F1 score for the Non-BrS category are 0.69, 0.75, and 0.72 respectively. As shown by the confusion matrix, out of 101 Definitive category samples, 86 were accurately classified and 15 were wrongly classified. Similarly, out of 44 Non-BrS samples

The Area Under the Curve (AUC) for the ROC plot was 0.849, while the optimized decision boundary came to about 0.39. The ECDF plot revealed the effects of the use of weighted sampling while training, while the attention plots gave us some intuition about how our model operates.

It has been demonstrated that the algorithm is quite capable of detecting patterns of Brugada Syndrome Type 1 from digitized ECG recordings with an acceptable level of accuracy. On the other hand, the presence of both false positives and false negatives suggests that improvements to the system are still needed. The next chapter gives a thorough analysis of the results obtained.

Chapter 6

Discussion

6.1 Introduction

In this chapter, we will analyze the outcomes that have been obtained through the CNN-BiLSTM-Attention model, which is used to diagnose Type 1 Brugada syndrome from digitized electrocardiograms. While Chapter 5 provided numerical output, confusion matrices, ROC analysis, and attention maps, this chapter gives a technical and clinical insight into these outputs.

The test accuracy rate for the system is 82%. The model achieved better results in detecting the Definite / Brugada Type 1, where its precision is 0.89, recall rate is 0.85, and F1 score is 0.87. On the other hand, for the non-BrS class, the model returned 0.69 in precision, 0.75 in recall, and an F1-score of 0.72. This shows that the model was capable of extracting significant ECG morphology features related to Brugada Type 1.

The discussion above is justified since simply having accuracy is not enough in this case. False negative and false positives have different implications. The former might miss out on identifying a genuine Type 1 ECG pattern while the latter can make clinicians waste their time in conducting a review that is unnecessary. As such, the model must be reviewed on its strengths and limitations.

6.2 Interpretation of the Main Results

From the results, the model exhibited good performance in detecting Type 1 Brugada pattern automatically. With an overall accuracy of 82%, this implies that most of the test ECG windows were successfully recognized. However, owing to the unbalanced nature of the dataset, class-wise analysis would be more insightful.

The best performing class was Definitive/Brugada Type 1. The classification results show that the model was able to classify correctly 86 out of 101 cases in the

Definitive class, which suggests that the model recognizes ECG features associated with the Brugada Type 1 morphology. Since the main focus of this thesis work was to detect the Definitive class, these results are promising.

The overall accuracy rate of the Non-BrS group was relatively low. The model was able to predict 33 out of 44 Non-BrS windows correctly, while 11 windows in the Non-BrS group were incorrectly assigned into the Definitive category. This may be due to the low number of samples used for Non-BrS cases or their similar appearance with Brugada-like ECG patterns.

The ROC-AUC score of 0.849 confirms the efficiency of the model to classify the two classes. The optimal threshold of 0.39 helped to balance the tradeoff between predicting Brugada Type 1 and reducing the false positives.

6.3 Clinical Meaning of the Results

The accuracy of the Definitive class is of clinical relevance since Type 1 Brugada pattern is regarded as the definitive ECG finding in Brugada Syndrome. The 0.85 recall score implies that the classifier recognized most of the Definitive cases. This is clinically relevant due to the possibility that the absence of Type 1 Brugada pattern on the ECG may delay further diagnosis or treatment.

The value of 0.89 means that the most number of windows classified as Definitive is Definitive indeed. It is a good indication of the accuracy of the model in making positive classifications. However, 15 instances of false negatives indicate that the system is still not ready to be used as a sole decision-making process.

From the standpoint of medical practice, the model should be regarded as a decision support system. Such a system can help identify suspicious ECG windows for further analysis by specialists, especially when the ECG data are extracted in digital form from PDF files. Nonetheless, the final diagnosis should always be made by professionals.

6.4 Effect of Class Imbalance

Class imbalance was one of the main issues with the research. Cleaned data had more Definitive cases compared to Non-BrS cases. This trend did not change even after the extraction of windows from the data. The resulting data had 1,832 Definitive windows and 545 Non-BrS windows.

This imbalance can cause the classifier to learn the majority class in particular. This means that it is more likely to predict uncertain cases as belonging to the Definitive class. It accounts for the superior results obtained by the Definitive class when compared to the Non-BrS class.

In order to address this issue, the training pipeline adopted WeightedRandomSampler. In doing so, it was possible to be exposed to a class distribution that would prove more representative. However, sampling based on weights cannot be considered as a replacement for data diversity. For future research, there is a need to include more examples of non-BrS cases in order to improve the capability of differentiating ECGs.

6.5 Threshold Optimization and Attention Maps

The optimized decision threshold of about 0.39 was used based on ROC and Youden's J index calculations. The threshold is less than the typical threshold of 0.5; this allows an improvement in sensitivity to detect Definitive. When screening, the higher sensitivity due to use of lower thresholds might prove beneficial because the risk of missing out on a Definitive patient would be greater than that of a false positive.

Attention maps were used in order to increase transparency. With the ECG windows aligned to the S-peak of the ECG signal, the attention maps helped identify the sections of the ECG signal that were used by the algorithm in order to make decisions. In the case of detecting the Brugada Type 1 pattern, the most important section is supposed to be the QRS-ST-T complex, especially the J-point, ST segment, and T wave.

Attention maps need to be interpreted carefully. Attention maps cannot prove that the neural network uses the same reasoning process as a cardiologist. The attention map only provides visual support to back up the claims about how the network works. Further studies must compare the attention maps against the annotations by cardiologists.

6.6 Strengths of the Proposed Pipeline

One of the major strengths of this thesis is its demonstration of the complete pipeline. Instead of starting with an existing digital version of the ECG data, in this thesis, the data was first extracted from PDF form, cleaned up, organized, and processed before being used to train the neural networks. The practicality of this method is increased by the fact that many medical ECGs exist in PDF form.

The second advantage comes from the preprocessing method which is based on the clinical knowledge. Namely, the classifier focuses on three leads, V1, V2, and V3, which were recognized as the most relevant leads to detect Brugada Type 1 syndrome. The usage of the S-peak centered window guarantees that the classifier receives QRS-ST-T wave complex.

This architecture is suitable for ECG classification. Convolutional layers are used to extract local patterns, while BiLSTM layers take into account temporal relationships between data points. The introduction of the attention module provides visualization capability. Another improvement is achieved by employing weighted sampling and threshold optimization techniques.

6.7 Limitations of the Study

However, despite having achieved some positive outcomes, there are also some weaknesses associated with this research. The first weakness that should be highlighted is related to data set size and imbalance, since there were fewer cases of non-brs than cases of definitive, which is affected class wise performance. A larger and more balanced dataset would likely improve model generalization.

A second weakness is that of the quality of digitization. As the data for the ECG came in PDF form, the process of digitizing could have introduced errors due to factors such as grid interference, differences in scale, quality of the image, and accuracy in wave-form tracing. These could influence the morphology of the ECG used in the study.

Another constraint is the fact that the model uses only leads V1, V2, and V3. Even though these leads are important for diagnosing Brugada type 1, there are other leads like II, III, and aVF that may prove useful. There can be future research on the effectiveness of including them.

The classifier model was confined to a binary approach, where ECGs were classified into Definitive or Non-BrS groups. However, in actuality, patterns of borderlines, Type 2, and Brugada phenocopies can also be seen. Thus, a possible development would be incorporating multi-class classification into the algorithmic model.

Lastly, there has been no external validation performed. The results are based on the existing data and the internal testing division. In order to use it in practice, external validation is needed using other ECG sources.

6.8 Future Improvements

Future research should start off by concentrating on increasing the dataset size and diversity, especially that of the Non-BrS category. Adding more ECG samples from patients who do not suffer from Brugada syndrome will be a step toward minimizing false positives.

Validation on an external basis is equally important. Validation using electrocardiograms collected from varied hospitals and patient samples would show the generalizability of the model outside the current data set.

Further improvement to this can be achieved by using additional ECG leads. Although the best leads used to detect Brugada Type 1 are V1-V3, there are other inferior leads that may give some additional support. Future research can incorporate V1-V3 leads against a 6 lead system or even 12 lead system.

The digitization procedure can be made more effective by automating the elimination of grids, improving waveform acquisition, and conducting rigorous signal quality evaluation. Ineffectively obtained ECGs can be rejected before any learning takes place.

Thirdly, the interpretability of the results could also be improved through the comparison of attention maps with regions identified by cardiologists in the ECG. In particular, the model should focus on relevant features, including the J point, the ST segment, and the T wave.

6.9 Chapter Summary

The results for the proposed CNN-BiLSTM-Attention model for detecting Type 1 Brugada Syndrome are presented in this chapter. The overall accuracy rate was achieved at 82%, with impressive results being observed in the Definitive category. These results show that the model learned relevant ECG patterns related to Brugada Syndrome Type 1.

These were emphasized in terms of the effects of the imbalance in classes, threshold tuning, and attention maps. The main strengths of this pipeline include electrocardiogram digitization using PDF files, preprocessing based on clinical aspects, use of the S-peak-centered windowing approach, multi-lead input data, use of deep learning, and visual assessment.

However, there are certain limitations associated with this study, which include data imbalance, digitization of the features, limited lead usage, binary classification, and lack of external validation. Consequently, the suggested approach can be considered a preliminary solution for further investigation but not a final diagnostic tool.

Chapter 7

Conclusion and Future Work

7.1 Introduction

The conclusion of this thesis is provided in this chapter where all the work performed for the development of an automated detection system for Brugada Syndrome Type 1 using the digitized ECG signals and deep learning techniques is described in detail. In essence, the thesis puts forth an end-to-end framework that commences from the ECG records stored in the form of PDF documents to produce the required CNN-BiLSTM-Attention classifier.

In the development of the thesis, there were two main goals: first, to design a neural network; second, to solve the problem of preparing real-world ECG datasets for use in training an artificial neural network. Since the original ECG signals came in the form of PDF files, their processing was necessary before training.

Conclusion: The final results showed very good performance for the Definitive / Brugada Type 1 category. The test accuracy achieved was 82%, while the Definitive class achieved a precision, recall, and f1-score of 0.89, 0.85, and 0.87, respectively. From these results, we can conclude that the model learned important information from the ECG regarding the Type 1 Brugada diagnosis.

7.2 Summary of the Thesis

The focus of the study will be on the identification of Type 1 Brugada Syndrome, otherwise referred to as Definitive ECG pattern. This study began with the provision of electrocardiogram readings in PDF files. The electrocardiograms could not be used directly for the purposes of machine learning since they consisted of graphical representations of the signals.

ECGD was used to digitize the ECG in order to solve the problem. The PDFs of the ECGs were transformed into numeric XLSX files. The combined dataset of

raw digitized data included 1,041 XLSX files. After labeling and preprocessing of the data, 784 labeled ECGs were left in the dataset, with 610 Definitive and 174 Non-BrS files.

ECG datasets went through pre-processing steps. More specifically, leads V1, V2, and V3 were used since they carry clinical significance towards detecting Brugada Type 1. Signal processing was done by resampling at 500 Hz, cleaning, and windowing according to the position of S-peaks. The selected window was able to cover QRS-ST-T segment, which contains the morphological information of Brugada Type 1.

Lastly, a CNN-BiLSTM-Attention structure was used for binary classification tasks. This network utilized convolutional networks to learn local ECG features, bi-LSTM networks to detect temporal relationships, and an attention mechanism for interpretation purposes. Classification performance analysis of the proposed model was carried out via classification measures, confusion matrix, ROC curve, optimum threshold, sampling ECDF, and attention maps.

7.3 Main Contributions

The main contributions of the thesis are concluded in Table 7.1.

Table 7.1: Summary of main contributions

Contribution	**Description**
ECG digitization	Converted PDF ECG records into XLSX numerical signal files
Dataset construction	Cleaned 1041 raw XLSX files into 784 labeled ECG files
Clinical preprocessing	Used V1, V2, V3 leads and S-peak-centered ECG windows
Neural network model	Implemented CNN-BiLSTM-Attention architecture
Class imbalance handling	Used weighted sampling during training
Threshold optimization	Applied ROC-based Youden's J threshold selection
Interpretability	Used attention maps to visualize model focus
Evaluation	Used accuracy, precision, recall, F1-score, confusion matrix, and ROC-AUC

Such contributions indicate that the thesis is not just a classification effort but a biomedical engineering process, which includes ECG digitalization and predictions

using AI.

7.4 Conclusion from Results

The final model had an overall test accuracy of 82%. With regard to the Definitive/Brugada Type 1 category, the precision of the model was found to be 0.89, recall was 0.85, and F1 score was 0.87. This shows that the model was able to predict most of the Brugada Type 1 ECGs accurately.

In the case of Non-BrS class, the precision was found to be 0.69, recall 0.75, and F1-score 0.72 for the model. In comparison to other two categories, the accuracy has been observed to be somewhat poor due to relatively fewer sample sizes available for Non-BrS category. There were 11 false positive values along with 15 false negative values too.

A high ROC-AUC value of 0.849 shows that there is a high discriminatory power within the model. With the optimum cut-off point of around 0.39, we have improved our decision boundary compared to the threshold value of 0.5.

The conclusions made from the research suggest that digital ECG recordings can be successfully used with deep learning algorithms to diagnose Brugada Syndrome Type 1. However, the current system is recommended to be considered as an experimental prototype only and not as an official diagnosing tool.

7.5 Future Work

Future research needs to first consider increasing the amount of data samples and their diversity, especially for the Non-BrS category. Increasing the number of non-BrS ECGs would be beneficial as it would reduce the incidence of false positives.

The validation process must be done externally as well. It will have to undergo evaluation through ECG measurements from hospitals and patients across a wide range of ECG machines and demographics.

Another improvement that could be made includes the use of additional ECG leads. Although this thesis deals with leads V1, V2, and V3, future research could include leads II, III, and aVF, or even the complete set of 12-lead ECG leads.

Multi-class classification could be considered beyond binary classification. In the future, other models will classify ECGs into Non-BrS, Borderline, and Definitive classes.

There is potential to enhance the digitization procedure through grid removal, better waveform detection, and evaluation of signal quality. In addition, attention maps need to be compared with annotations made by cardiologists.

7.6 Final Remarks

In this thesis, an automated end-to-end pipeline is proposed to detect Brugada Syndrome Type 1 based on digitalized electrocardiogram (ECG) signals in combination with deep learning techniques. The pipeline started from converting ECG data in PDF format to numeric data signals, then organizing data for analysis including cleaning data and selecting relevant ECG segments. Finally, training and testing a CNN-BiLSTM-Attention network were done.

From the results, the proposed algorithm performed quite well especially when the Definitive/Brugada Type 1 was considered. The accuracy recorded for this class was 82% while the F1 score was 0.87.

Conclusion Overall, it has been proved that electrocardiogram recordings in PDF image form can be transformed into machine-readable data to be used for automatic recognition of Brugada Type 1. In the case of access to large data sets and better image digitization, further research in cooperation with clinicians may lead to building a reliable decision support tool based on ECGs.

Bibliography

[1] Darwin Labarthe. «Epidemiology and prevention of cardiovascular diseases: a global challenge». In: (2011).

[2] Lennart Bergfeldt. «Differential diagnosis of cardiogenic syncope and seizure disorders». In: *Heart* 89.3 (2003), pp. 353–358.

[3] Charles Antzelevitch, Pedro Brugada, Martin Borggrefe, et al. «Brugada Syndrome: Report of the Second Consensus Conference». In: *Circulation* 111.5 (2005), pp. 659–670.

[4] Pedro Brugada and Josep Brugada. «Right Bundle Branch Block, Persistent ST Segment Elevation and Sudden Cardiac Death: A Distinct Clinical and Electrocardiographic Syndrome». In: *Journal of the American College of Cardiology* 20.6 (1992), pp. 1391–1396.

[5] Liping Xie, Zilong Li, Yihan Zhou, Yiliu He, and Jiaxin Zhu. «Computational diagnostic techniques for electrocardiogram signal analysis». In: *Sensors* 20.21 (2020), p. 6318.

[6] Peter J Schwartz, Michael J Ackerman, Charles Antzelevitch, Connie R Bezzina, Martin Borggrefe, Bettina F Cuneo, and Arthur AM Wilde. «Inherited cardiac arrhythmias». In: *Nature reviews Disease primers* 6.1 (2020), p. 58.

[7] Antonio B. de Luna, Javier Garcia-Niebla, and Adrian Baranchuk. «New Electrocardiographic Features in Brugada Syndrome». In: *Current Cardiology Reviews* 10.3 (2014), pp. 175–180.

[8] Kayode S Adewole et al. «Expert system and decision support system for electrocardiogram interpretation and diagnosis: review, challenges and research directions». In: *Applied Sciences* 12.23 (2022), p. 12342.

[9] Monica De Gaspari, Stefania Rizzo, Gaetano Thiene, and Cristina Basso. «Causes of sudden death». In: *European Heart Journal Supplements* 25.Supplement_B (2023), B16–B20.

[10] Britt-Maria Beckmann, Arne Pfeufer, and Stefan Kääb. «Inherited cardiac arrhythmias: diagnosis, treatment, and prevention». In: *Deutsches Ärzteblatt International* 108.37 (2011), p. 623.

[11] Connie R Bezzina, Martin B Rook, and Arthur AM Wilde. «Cardiac sodium channel and inherited arrhythmia syndromes». In: *Cardiovascular research* 49.2 (2001), pp. 257–271.

[12] Esperanza Agullo-Pascual, Marina Cerrone, and Mario Delmar. «Arrhythmogenic cardiomyopathy and Brugada syndrome: diseases of the connexome». In: *FEBS letters* 588.8 (2014), pp. 1322–1330.

[13] Ana Mincholé, Julià Camps, Aurore Lyon, and Blanca Rodríguez. «Machine learning in the electrocardiogram». In: *Journal of electrocardiology* 57 (2019), S61–S64.

[14] Antoni Bayés De Luna. *Basic electrocardiography: normal and abnormal ECG patterns*. John Wiley & Sons, 2008.

[15] Paul-Adrian Călburean et al. «Predicting and Recognizing Drug-Induced Type I Brugada Pattern Using ECG-Based Deep Learning». In: *Journal of the American Heart Association* 13.10 (2024), e033148.

[16] Mehdi Imani, Majid Joudaki, Ayoub Bagheri, and Hamid R Arabnia. «Why ROC-AUC Is Misleading for Highly Imbalanced Data: In-Depth Evaluation of MCC, F2-Score, H-Measure, and AUC-Based Metrics Across Diverse Classifiers». In: *Technologies* 14.1 (2026), p. 54.

[17] Francesco Vitali et al. «Standard ECG in Brugada syndrome as a marker of prognosis: from risk stratification to pathophysiological insights». In: *Journal of the American Heart Association* 10.10 (2021), e020767.

[18] Cameron J Leong, Sohat Sharma, Jayant Seth, and Simon W Rabkin. «Artificial intelligence streamlines diagnosis and assessment of prognosis in Brugada syndrome: a systematic review and meta-analysis». In: *Connected Health And Telemedicine* 3.2 (2024), N–A.

[19] Silvia G. Priori, Arthur A. M. Wilde, Minoru Horie, et al. «Executive Summary: HRS/EHRA/APHRS Expert Consensus Statement on the Diagnosis and Management of Patients with Inherited Primary Arrhythmia Syndromes». In: *Heart Rhythm* 10.12 (2013), pp. 1932–1963.

[20] Souhaila Dari Berraha. «Machine learning-based classification of ECG biomark┤ers for Brugada syndrome diagnosis». In: (2024).

[21] Muhammad Wasimuddin, Khaled Elleithy, Abdel-Shakour Abuzneid, Miad Faezipour, and Omar Abuzaghleh. «Stages-based ECG signal analysis from traditional signal processing to machine learning approaches: A survey». In: *IEEE Access* 8 (2020), pp. 177782–177803.

[22] Shohreh Honarbakhsh et al. «A primary prevention clinical risk score model for patients with Brugada syndrome (BRUGADA-RISK)». In: *Clinical Electrophysiology* 7.2 (2021), pp. 210–222.

[23] Vincenzo Randazzo, Alessandro Casella, Silvia Caligari, Fiorenzo Gaita, Carla Giustetto, and Eros Pasero. «A Three-Class AI Model for Brugada Syndrome Detection to Improve Diagnostic Accuracy in ECG Analysis». In: *IEEE International Symposium on Medical Measurements and Applications (MeMeA)* (2025).

[24] Pasquale Crea, Giuseppe Picciolo, Francesco Luzza, and Giuseppe Oreto. «ST Segment Depression in the Inferior Leads in Brugada Pattern: A New Sign». In: *Annals of Noninvasive Electrocardiology* 20.6 (2015), pp. 561–565. DOI: 10.1111/anec.12247.

[25] Tom Fawcett. «An Introduction to ROC Analysis». In: *Pattern Recognition Letters* 27.8 (2006), pp. 861–874.

[26] Arthur A. M. Wilde, Charles Antzelevitch, Martin Borggrefe, et al. «Proposed Diagnostic Criteria for the Brugada Syndrome». In: *European Heart Journal* 23.21 (2002), pp. 1648–1654.

[27] Yann LeCun, Leon Bottou, Yoshua Bengio, and Patrick Haffner. «Gradient-Based Learning Applied to Document Recognition». In: *Proceedings of the IEEE* 86.11 (1998), pp. 2278–2324.

[28] Sepp Hochreiter and Jurgen Schmidhuber. «Long Short-Term Memory». In: *Neural Computation* 9.8 (1997), pp. 1735–1780.

[29] Dzmitry Bahdanau, Kyunghyun Cho, and Yoshua Bengio. «Neural Machine Translation by Jointly Learning to Align and Translate». In: *International Conference on Learning Representations*. 2015.

[30] Awni Y. Hannun, Pranav Rajpurkar, Masoumeh Haghpanahi, et al. «Cardiologist-Level Arrhythmia Detection and Classification in Ambulatory Electrocardiograms Using a Deep Neural Network». In: *Nature Medicine* 25 (2019), pp. 65–69.

[31] Antonio H. Ribeiro, Manoel H. Ribeiro, Gustavo M. M. Paixao, et al. «Automatic Diagnosis of the 12-Lead ECG Using a Deep Neural Network». In: *Nature Communications* 11 (2020), p. 1760.

[32] David M. W. Powers. «Evaluation: From Precision, Recall and F-Measure to ROC, Informedness, Markedness and Correlation». In: *Journal of Machine Learning Technologies* 2.1 (2011), pp. 37–63.

[33] Pranav Rajpurkar, Awni Hannun, Masoumeh Haghpanahi, et al. «Cardiologist-Level Arrhythmia Detection with Convolutional Neural Networks». In: *arXiv preprint arXiv:1707.01836* (2017).

[34] Yuka Mizusawa and Arthur A. M. Wilde. «Brugada Syndrome». In: *Circulation: Arrhythmia and Electrophysiology* 5.3 (2012), pp. 606–616.

[35] Juan Sieira and Pedro Brugada. «The Definition of the Brugada Syndrome». In: *European Heart Journal* 38.40 (2017), pp. 3029–3034.

[36] Pietro Delise, Giulia Allocca, and Nicoletta Sitta. «Risk Stratification in Individuals with the Brugada Type 1 ECG Pattern». In: *Journal of Cardiovascular Medicine* 12 (2011), pp. 408–412.

[37] Gari D. Clifford, Francisco Azuaje, and Patrick McSharry. *Advanced Methods and Tools for ECG Data Analysis*. Artech House, 2006.

[38] Leif Sornmo and Pablo Laguna. *Bioelectrical Signal Processing in Cardiac and Neurological Applications*. Elsevier Academic Press, 2005.

[39] Pablo Laguna, Raimon Jané, and Pere Caminal. «Automatic Detection of Wave Boundaries in Multilead ECG Signals». In: *Computers and Biomedical Research* 27.1 (1994), pp. 45–60.

[40] Jiapu Pan and Willis J. Tompkins. «A Real-Time QRS Detection Algorithm». In: *IEEE Transactions on Biomedical Engineering* 32.3 (1985), pp. 230–236.

[41] Dominique Makowski, Tam Pham, Zen J. Lau, et al. «NeuroKit2: A Python Toolbox for Neurophysiological Signal Processing». In: *Behavior Research Methods* 53 (2021), pp. 1689–1696.

[42] Ian Goodfellow, Yoshua Bengio, and Aaron Courville. *Deep Learning*. MIT Press, 2016.

[43] Ozal Yildirim. «A Novel Wavelet Sequence Based on Deep Bidirectional LSTM Network Model for ECG Signal Classification». In: *Computers in Biology and Medicine* 96 (2018), pp. 189–202.

[44] Serkan Kiranyaz, Turker Ince, and Moncef Gabbouj. «Real-Time Patient-Specific ECG Classification by 1-D Convolutional Neural Networks». In: *IEEE Transactions on Biomedical Engineering* 63.3 (2016), pp. 664–675.

[45] U. Rajendra Acharya, Hamido Fujita, Oh Shu Lih, et al. «Automated Detection of Arrhythmias Using Different Intervals of Tachycardia ECG Segments with Convolutional Neural Network». In: *Information Sciences* 405 (2017), pp. 81–90.

[46] Alex Graves and Jurgen Schmidhuber. «Framewise Phoneme Classification with Bidirectional LSTM Networks». In: *Proceedings of the International Joint Conference on Neural Networks* (2005), pp. 2047–2052.

[47] Ashish Vaswani, Noam Shazeer, Niki Parmar, et al. «Attention Is All You Need». In: *Advances in Neural Information Processing Systems*. 2017.

[48] Davide Chicco and Giuseppe Jurman. «The Advantages of the Matthews Correlation Coefficient over F1 Score and Accuracy in Binary Classification Evaluation». In: *BMC Genomics* 21 (2020), p. 6.

[49] Alan V. Oppenheim, Ronald W. Schafer, and John R. Buck. *Discrete-Time Signal Processing*. 2nd ed. Prentice Hall, 1999.

[50] Ilya Loshchilov and Frank Hutter. «Decoupled Weight Decay Regularization». In: *ICLR* (2019).

[51] W. J. Youden. «Index for Rating Diagnostic Tests». In: *Cancer* 3.1 (1950), pp. 32–35.

[52] Sarthak Jain and Byron C. Wallace. «Attention is not Explanation». In: *Proceedings of the 2019 Conference of the North American Chapter of the Association for Computational Linguistics (NAACL)*. Association for Computational Linguistics, 2019, pp. 3543–3556.